2020 Spring

Advanced Solidification

05.04.2020

Eun Soo Park

Office: 33-313
Telephone: 880-7221
Email: espark@snu.ac.kr
Office hours: by appointment

Binary phase diagrams

Contents for previous class
Solid-Liquid Equilibrium in Alloys

1) Simple Phase Diagrams

Both are ideal soln. → At T change, curvature and width change of G curve by S

2) Systems with miscibility gap

$\Delta H^{L}_{mix} = 0 \quad \Delta H^{S}_{mix} > 0$

At T change, curvature and width change of G curve by S + shape change of curve by H

4) Simple Eutectic Systems

$\Delta H^{L}_{mix} = 0 \quad \Delta H^{S}_{mix} >> 0$

→ miscibility gap extends to the melting temperature.

3) Ordered Alloys

$\Delta H^{L}_{mix} = 0 \quad \Delta H^{S}_{mix} < 0$

$\Delta H_{mix} < 0$ → A atoms and B atoms like each other. → Ordered alloy at low T

$\Delta H_{mix} << 0$ → The ordered state can extend to the melting temperature.

$\Delta H^{\alpha}_{mix} > \Delta H^{l}_{mix} > 0$

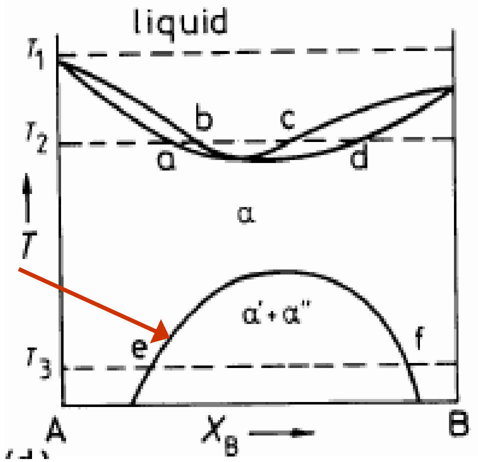

miscibility gab

$\Delta H^{\alpha}_{mix} < \Delta H^{l}_{mix} < 0$

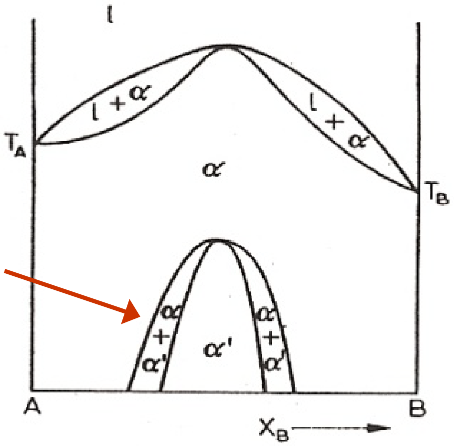

Ordered phase

Eutectic reaction

Considerable difference between the melting points

$$\Delta H_{mix}^{\alpha} > \Delta H_{mix}^{l} > 0$$

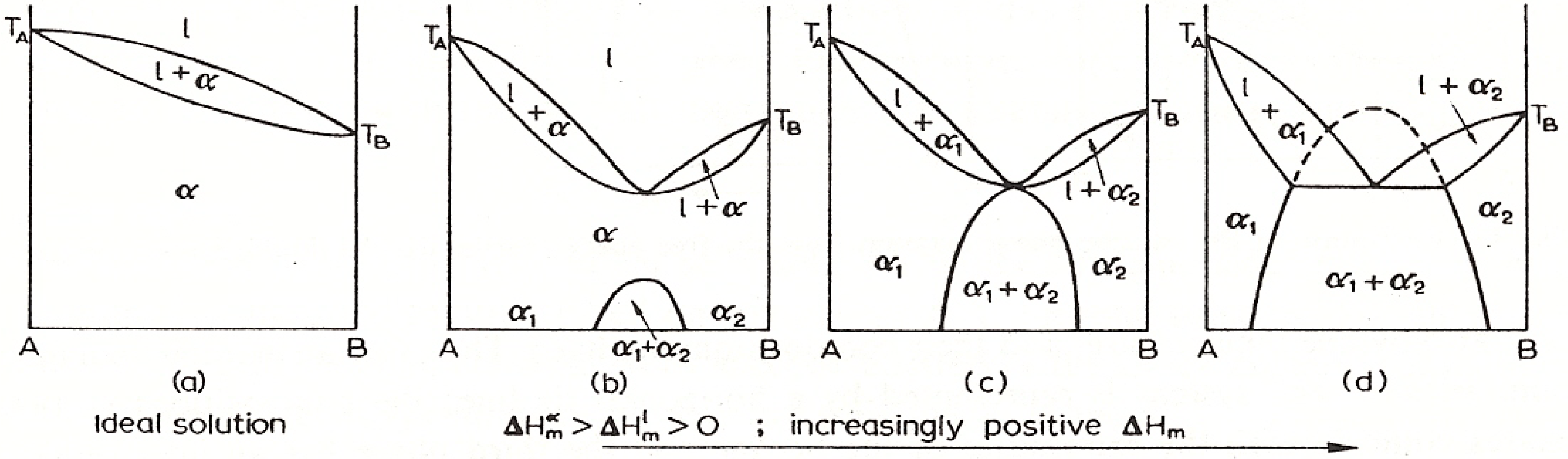

Fig. 43. Effect of increasingly positive departure from ideality in changing the phase diagram for a continuous series of solutions to a eutectic-type.

Peritectic reaction

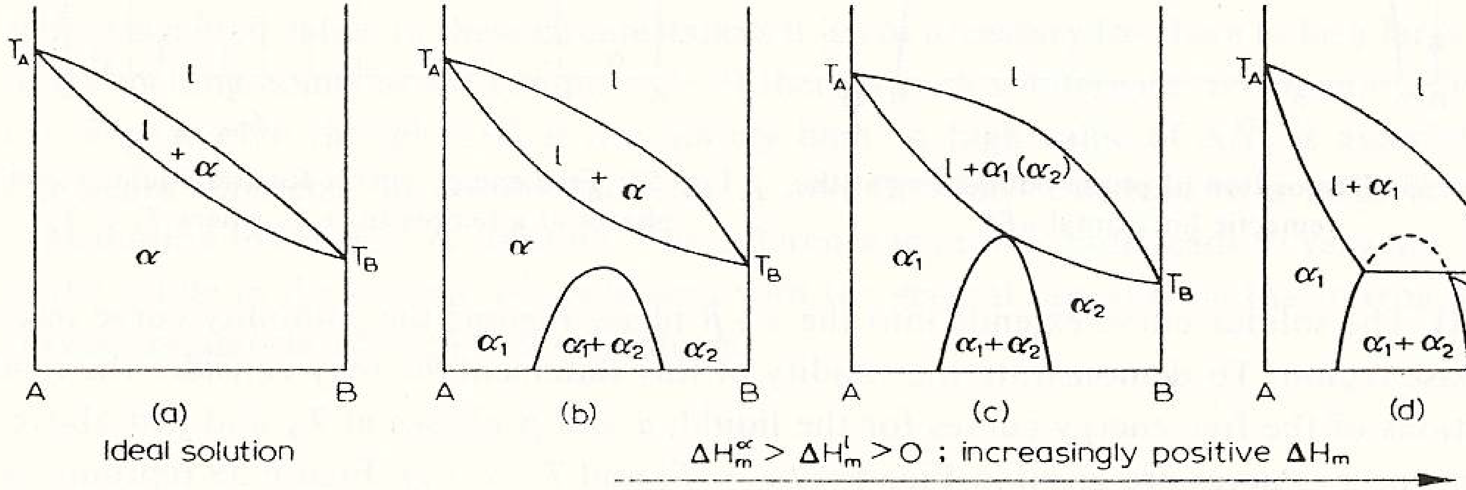

Fig. 61. Effect of increasingly positive departure from ideality in changing the phase diagram from a continuous series of solutions to a peritectic-type.

1.5 Binary phase diagrams

Intermediate Phase

*** Solid solution**

→ random mixing

→ entropy ↑

negative enthalpy ↓

$$\boxed{\Delta H^{S}_{mix} < 0}$$

Wide compositional range

➔ G ↓

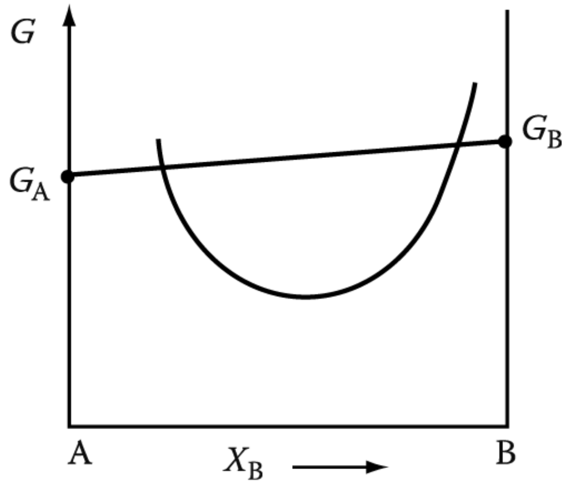

(b)

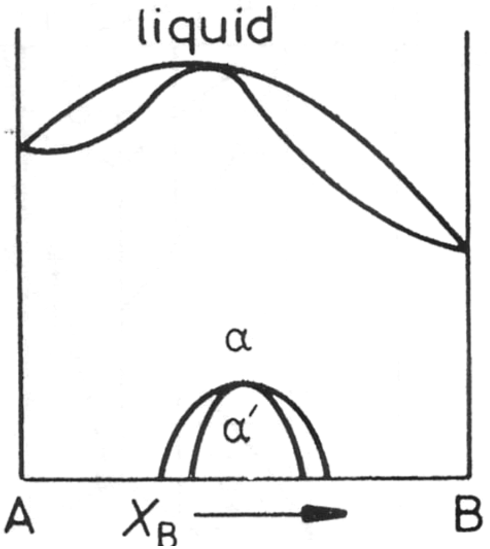

*** Compound : AB, A_2B…**

→ entropy↓

→ covalent, ionic contribution

→ enthalpy more negative ↓

$$\boxed{\Delta H^{S}_{mix} << 0}$$

Narrow compositional range

➔ G ↓

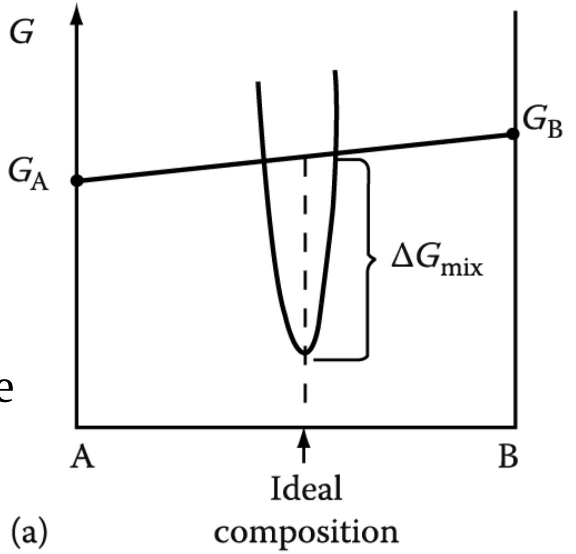

(a)

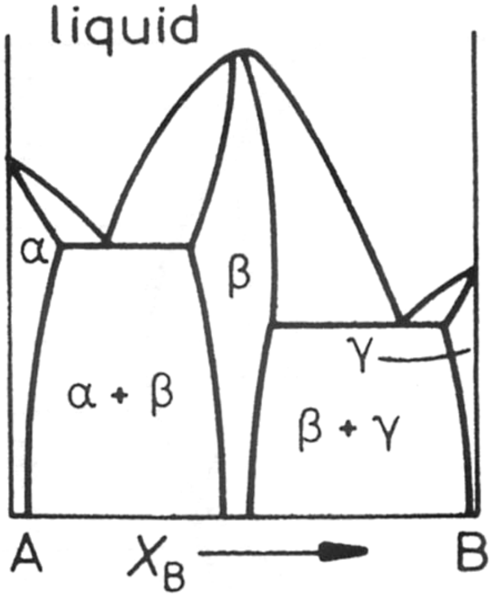

2.6 Origin of Defects

Microstructure is the collection of defects in the materials.

- ***Imperfection*** in Metallic Materials ;

Point defect : Vacancies, interstitials, Impurities

Line defect : Dislocations, Cellular and lineage substructure

Plane defect : Grain Boundaries, Free Surfaces

Bulk defect : Voids, Cracks

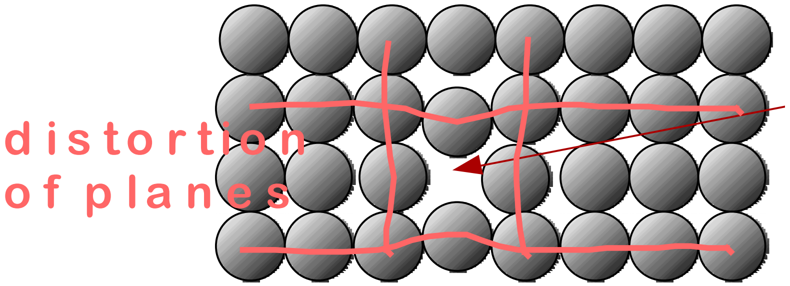

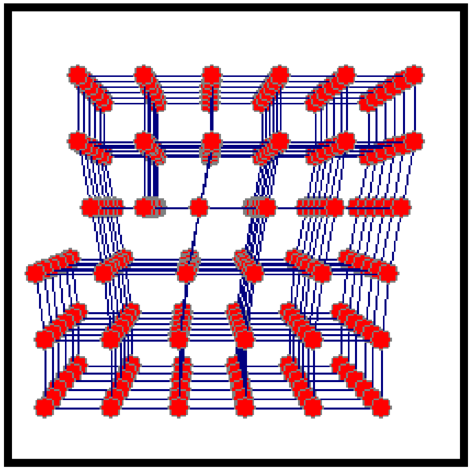

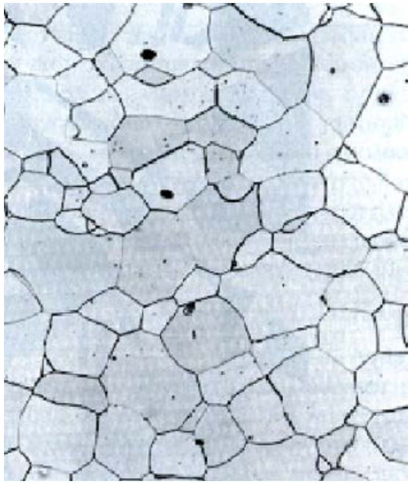

Heterogeneous Nucleation

Heterogeneous nucleation must occur on some substrate:

grain boundaries
triple junctions
dislocations
(existing) second phase particles

Consider a grain boundary: why is it effective?

Answer: by forming on a grain boundary, an embryo can offset its "cost" in interfacial energy by eliminating some grain boundary area.

Equilibrium concentration X_V^e will be that which gives the minimum free energy.

at equilibrium $\left(\frac{dG}{dX_V}\right)_{X_V = X_V^e} = 0$

$$\Delta H_V - T\Delta S_V + RT \ln X_V^e = 0$$

A constant ~3, independent of T

Rapidly increases with increasing T

$$X_V^e = \boxed{\exp\frac{\Delta S_V}{R}} \cdot \exp\frac{-\Delta H_V}{RT}$$

putting $\Delta G_V = \Delta H_V - T\Delta S_V$

$$\boxed{X_V^e = \exp\frac{-\Delta G_V}{RT}}$$

- **In practice, ΔH_V is of the order of 1 eV per atom and X_V^e reaches a value of about 10^{-4}~10^{-3} at the melting point of the solid**

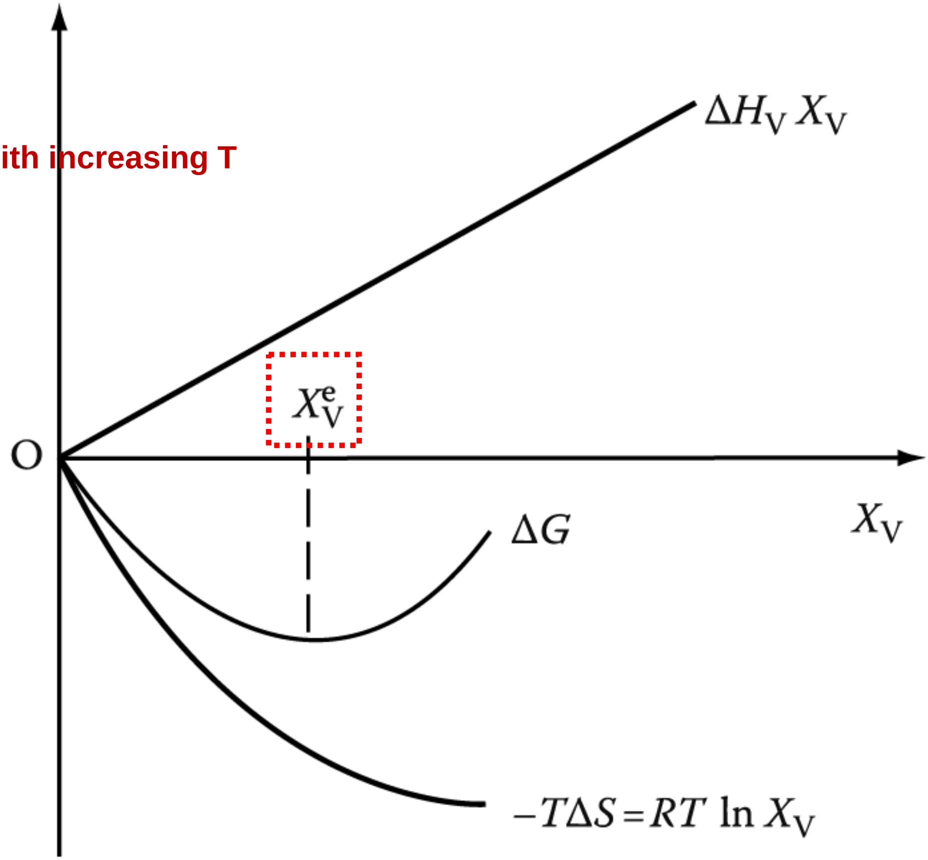

Fig. 1.37 Equilibrium vacancy concentration.

: adjust so as to reduce G to a minimum

c) Quenched-in Vacancies

In the vicinity of grain boundaries on subsequent aging,

Precipitate-Free Zone(PFZ) due to Vacancy Diffusion during quenching

Solute concentration within the zone ~ largely unchanged, but no precipitate at GB
∵ a critical vacancy supersaturation must be exceeded for nucleation to occur.

$$X_V^e = \exp\frac{-\Delta G_V}{RT}$$

$T \uparrow \Rightarrow X_V^e \uparrow$

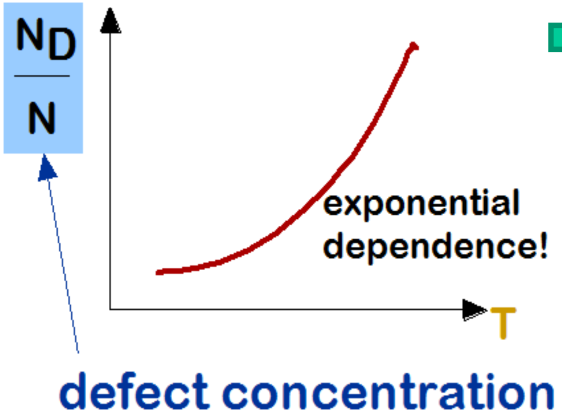

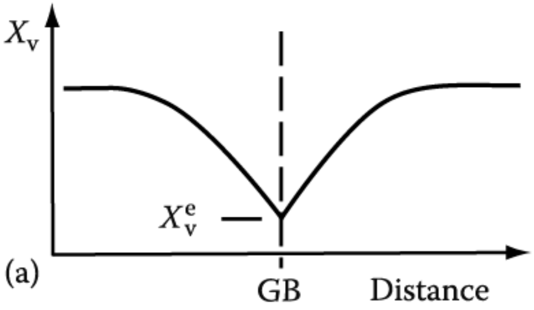

Similar PFZs can also form at inclusions and dislocations.

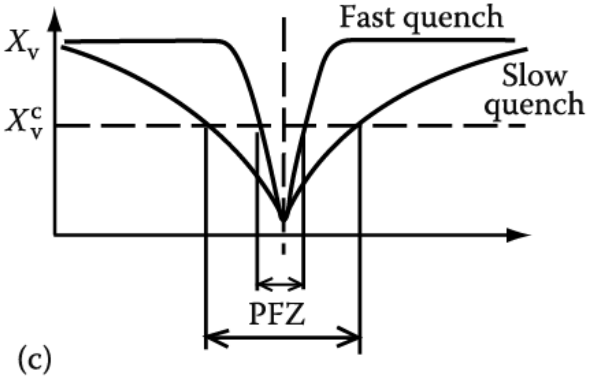

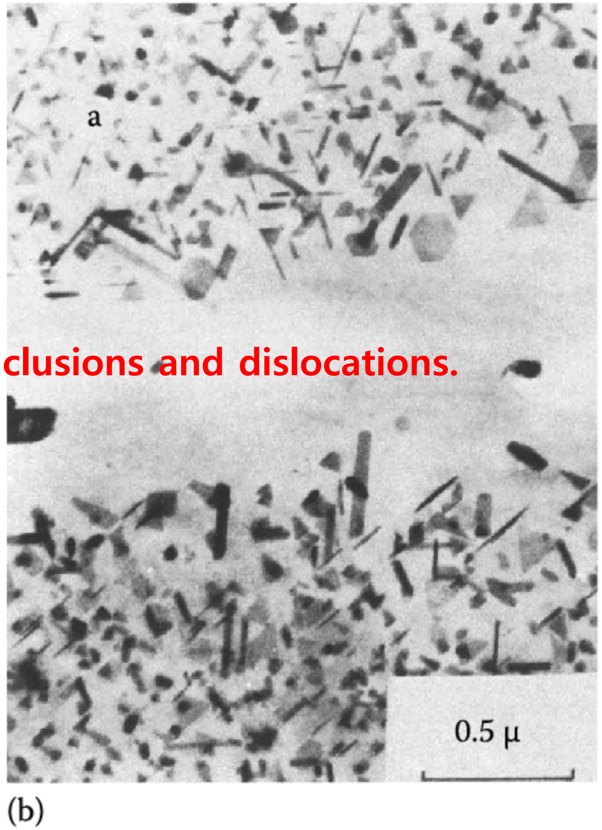

Fig. 5.35 A PFZ due to vacancy diffusion to a grain boundary during quenching.
(a) Vacancy concentration profile. (b) A PFZ in an Al-Ge alloy (x 20,000)
(c) Dependence of PFZ width on critical vacancy concentration X_v^c and rate of quenching.

⑤ Stresses due to inclusions. (dislocation density ~ inclusion density)

Coherency Loss

Precipitates with coherent interfaces = low interfacial E + coherency strain E

Precipitates with non-coherent interfaces = higher interfacial E

$$\Delta G(coherent) = 4\mu\delta^2 \cdot \frac{4}{3}\pi \boxed{r^3} + 4\pi \boxed{r^2} \cdot \gamma_{ch} \Leftrightarrow \Delta G(non-coherent) = 4\pi \boxed{r^2} \cdot (\gamma_{ch} + \gamma_{st})$$

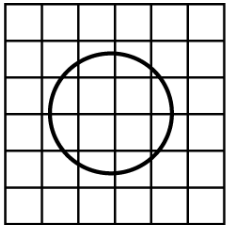

Coherency strain energy
Eq. 3.39

Chemical interfacial E

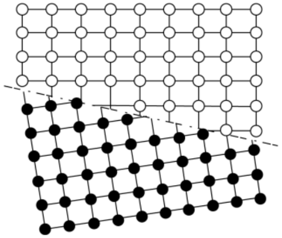

Chemical and structural interfacial E

$$\frac{4}{3}\pi r^3 (4\pi\mu\delta^2) + 4\pi r^2 (\gamma_{ch}) = 4\pi r^2 (\gamma_{st} + \gamma_{ch})$$

coherent ΔG_s-relaxed

$$\therefore \boxed{r_{crit} = \frac{3 \cdot \gamma_{st}}{4\mu\delta^2}}$$

$$\approx \frac{1}{\delta}$$ **($\delta = (d_\beta - d_\alpha)/ d_\alpha$: misfit)**

$$for\ small\ \delta, \quad \gamma_{st} \propto \delta$$

(semicoherent interface)

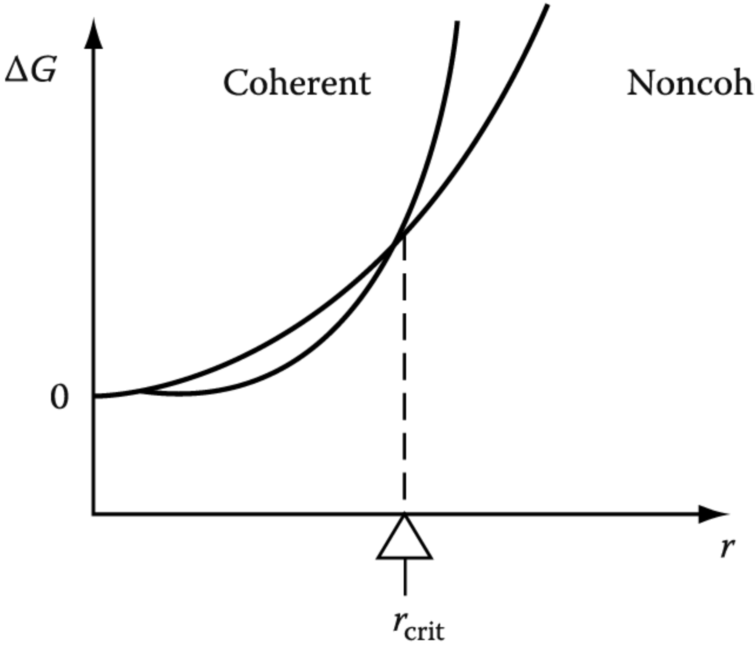

Fig. 3. 52 The total energy of matrix + precipitate vs. precipitate radius for spherical coherent and non-coherent (semicoherent of incoherent) precipitates.

⑥ Growth error: inherent feature

Liquid ↔ Solid transformation at T_m

Chapter 1: Equilibrium consideration (Thermodynamics)

Chapter 2: Atomic mechanism (Kinetics)

Chapter 3. Nucleation

3.1. Metastability of Supercooled Liquid

Solidification:

Liquid → Solid

↓

Presence of metastable supercooled liquid

Why?

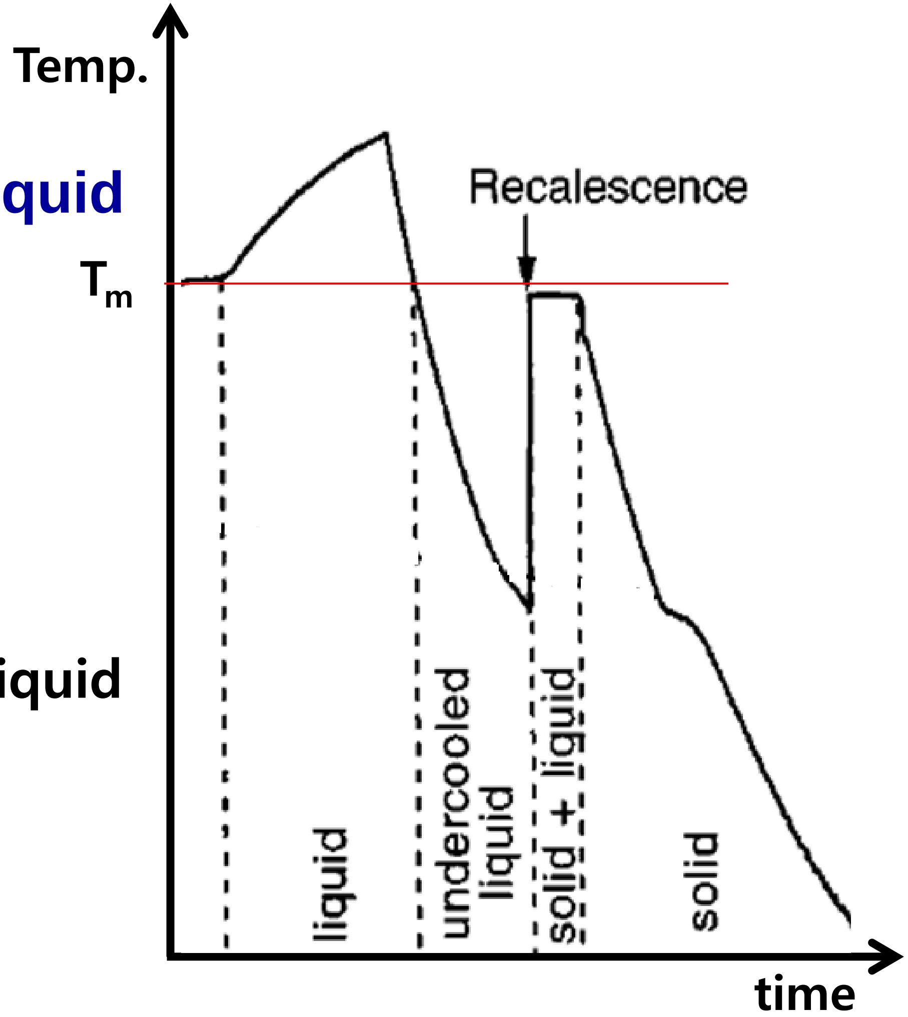

Turnbull's Insight for Supercooling

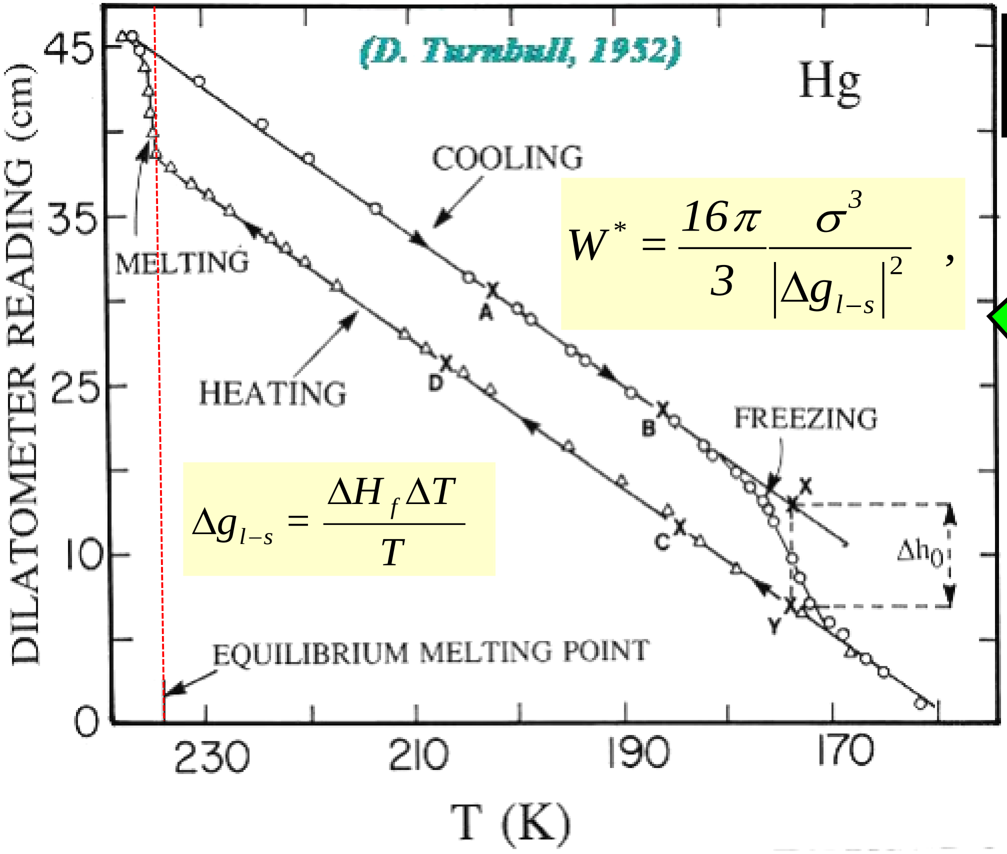

$$W^* = \frac{16\pi}{3}\frac{\sigma^3}{\left|\Delta g_{l-s}\right|^2},$$

$$\Delta g_{l-s} = \frac{\Delta H_f \Delta T}{T}$$

Microcrystalline structure for liquid metals
–*<u>Same short range order with crystals</u>*!

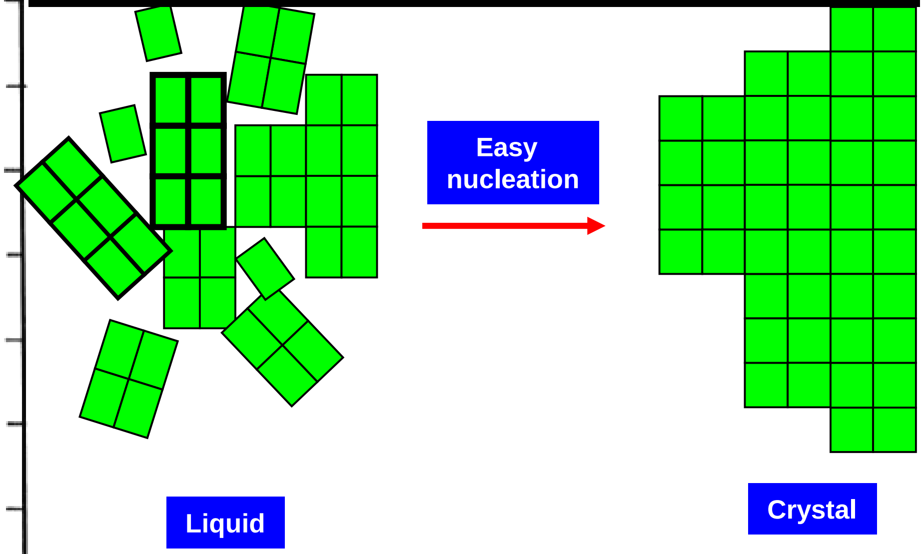

- ◆ <u>How</u> does the liquid metals resist on the crystallization?
- ◆ What is the origin of high nucleation barrier against the crystallization?
- → What is <u>the structure of interface</u> between liquids and crystals?
- ◆ What is the local order of liquid metals?

Turnbull’s solid-liquid interface

<u>Turnbull’s insight :</u> Liquid orders substantially near a crystal surface due to entropy decreasing caused by the crystal-melt interfacial tension

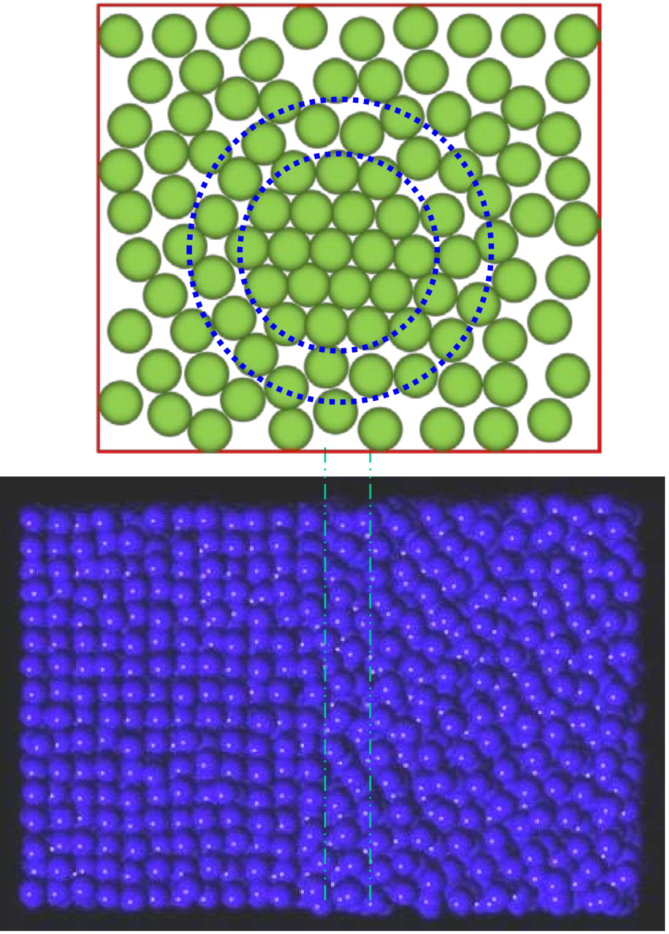

Solid state physics v47, 1 (1994)

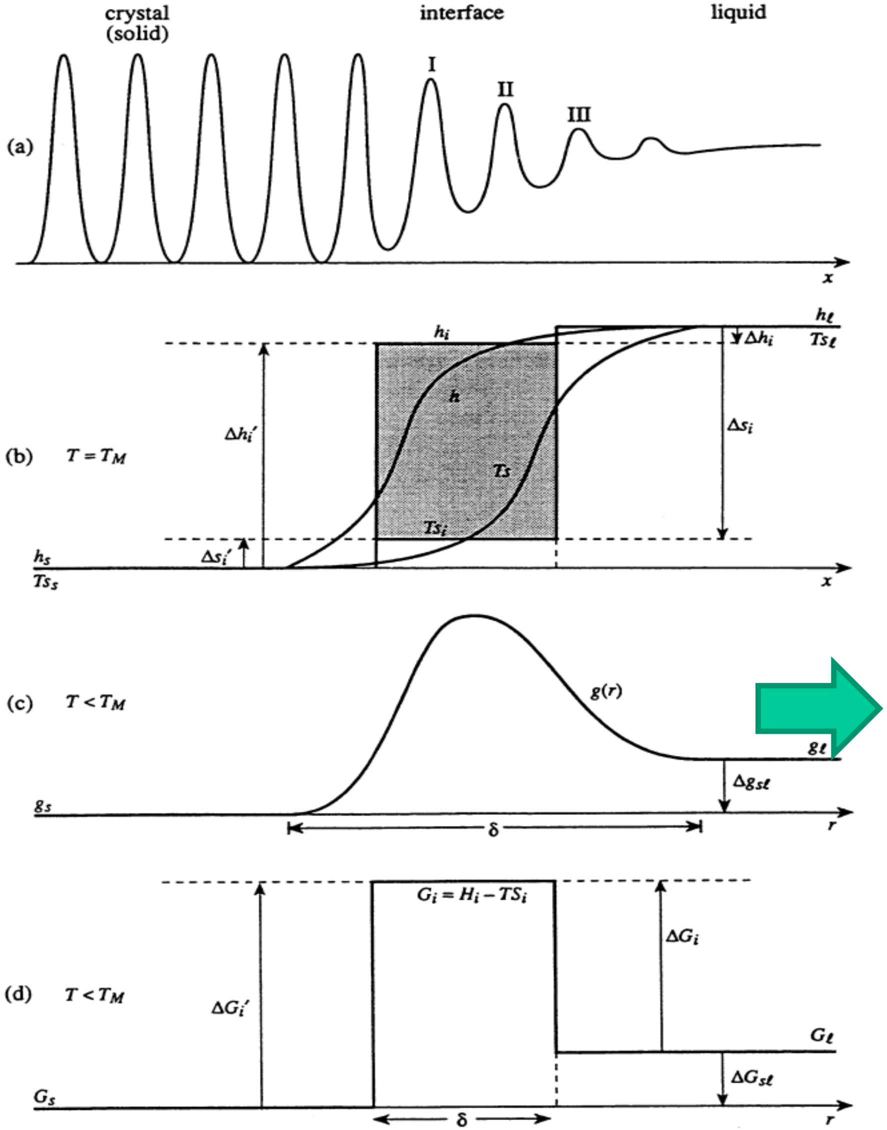

Supercooling

How to Obtain Extensive Undercooling

John H. PEREPEZKO, MSE, 65 (1984) 125-135

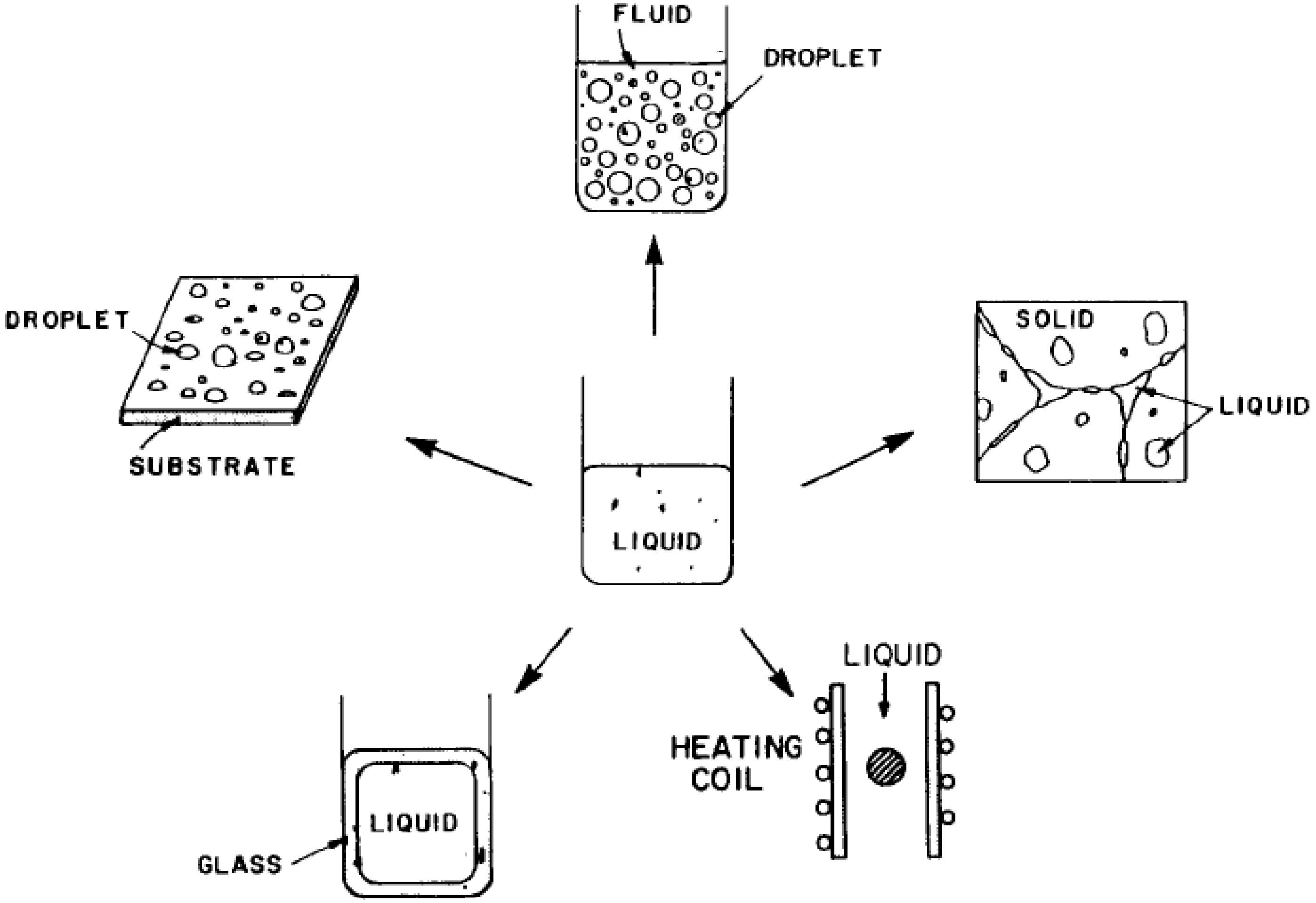

By dispersing a liquid into a large number of small droplets within a suitable medium, the catalytic effects of active nucleants may be restricted to a small fraction of the droplets so that many droplets will exhibit extensive undercooling.

Containerless and Contactless Measurement System

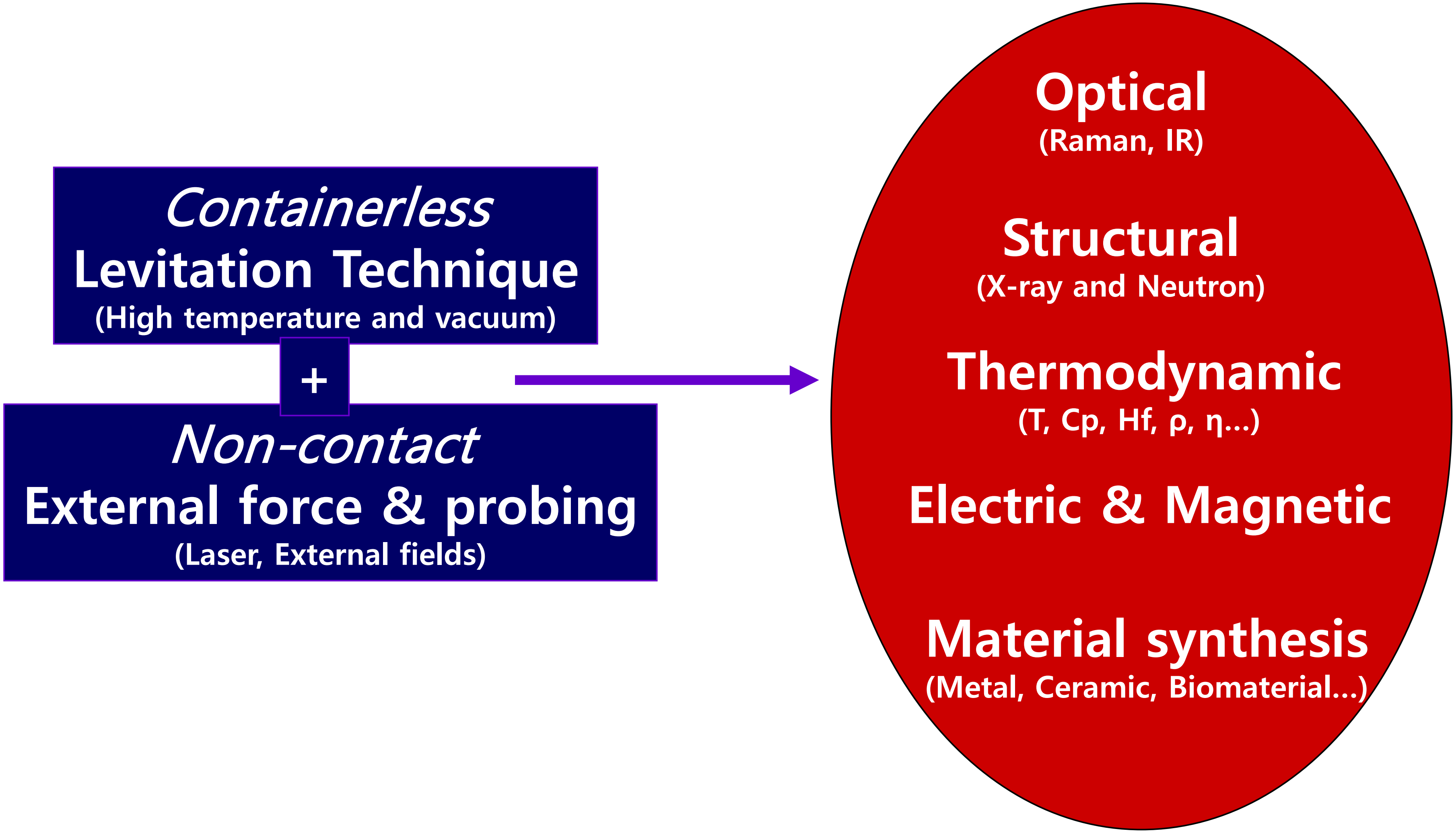

Containerless
Levitation Technique
(High temperature and vacuum)

\+

Non-contact
External force & probing
(Laser, External fields)

Optical
(Raman, IR)

Structural
(X-ray and Neutron)

Thermodynamic
(T, Cp, Hf, ρ, η…)

Electric & Magnetic

Material synthesis
(Metal, Ceramic, Biomaterial…)

High Temperature Levitation

Ultra-high temperature > 3000 ^{o}C

*** Magnetic/diamagnetic/superconducting levitation** → Only magnetic sample, below T_c

Acoustic

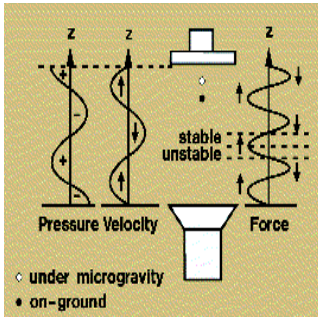

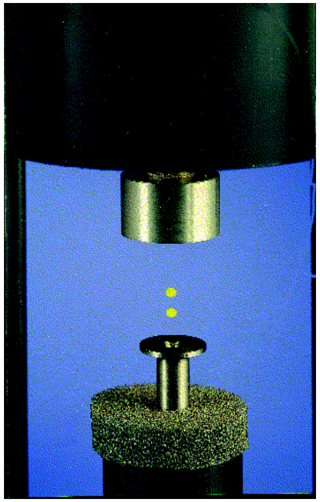

Requirement of acoustic media, Unstable at high T

Electrostatic

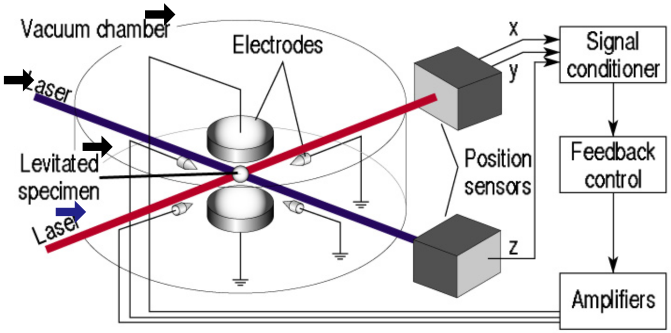

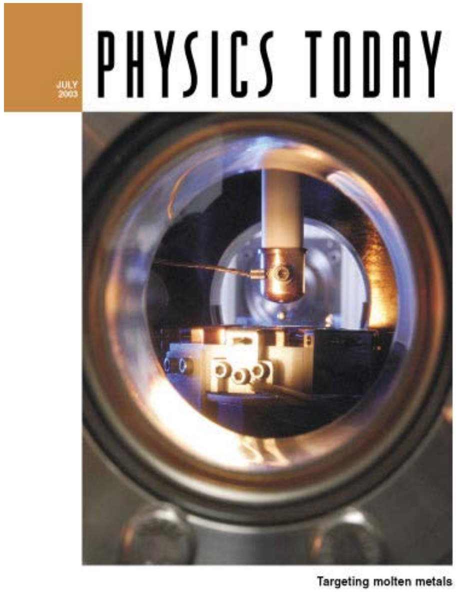

Physics Today, v56, p22, July 2003

All types of samples,
Suitable for sample heating

Electromagnetic

Only metallic & large mass sample

Aerodynamic

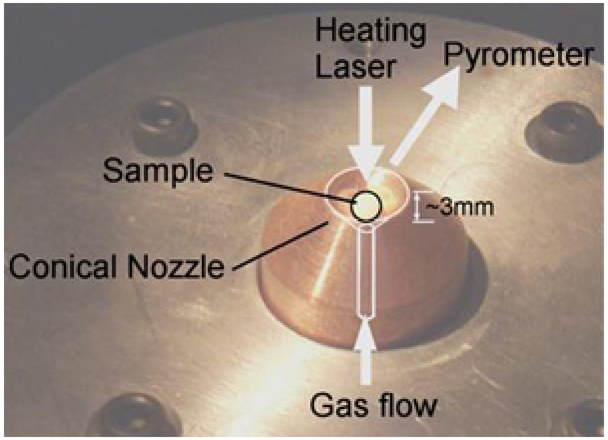

http://ec.europa.eu/research/industrial_technologies/articles/article_2288_en.html

Difficult to control rotation of sample,
Gas-sample reaction

Electrostatic Levitation (NASA, MSFC (Huntsville))

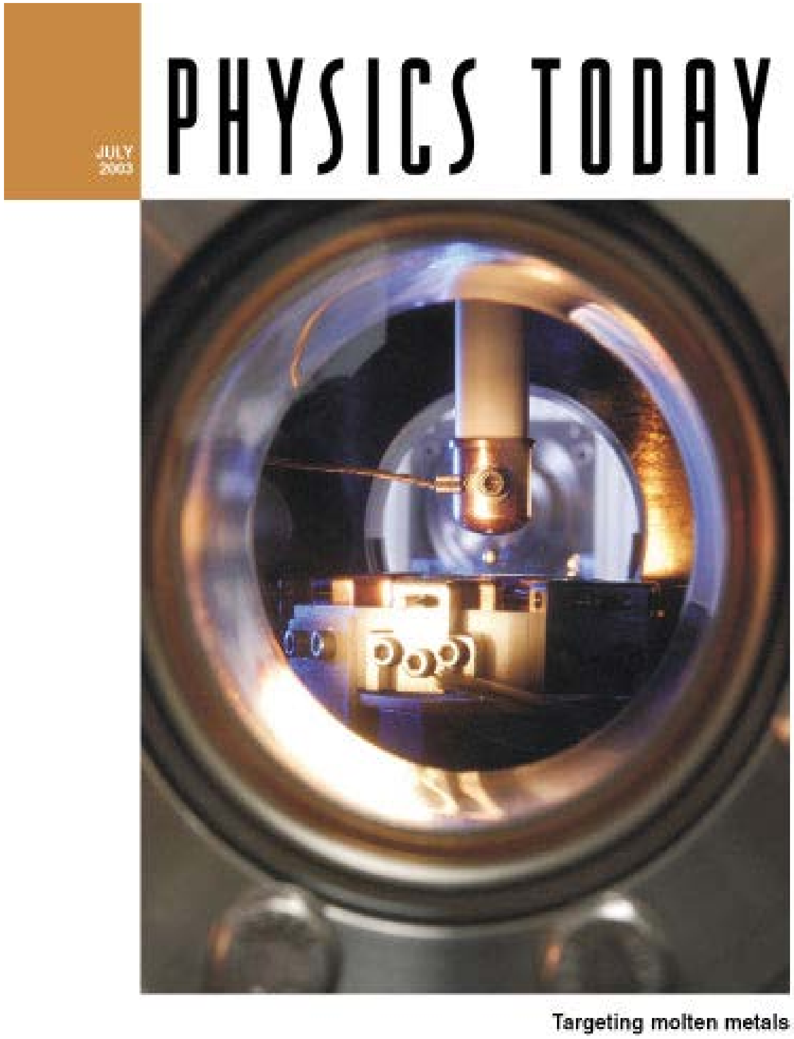

PHYSICS TODAY

JULY 2003

Targeting molten metals

Physics Today, v56, p22, July 2003

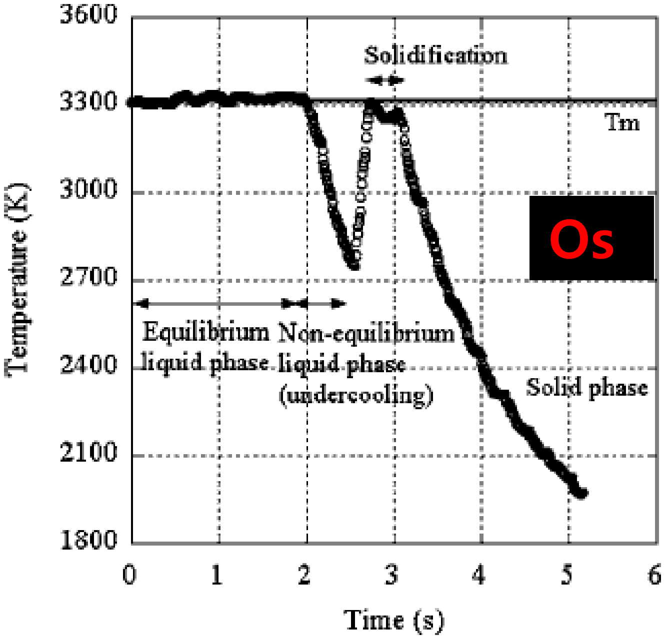

P.–F. Paradisa, et.al., JOURNAL OF APPLIED PHYSICS 100, 103523 2006

- **Specific heat,**
- **Emissivity,**
- **Density,**
- **Viscosity,**
- **Surface tension...**

Beam-ESL; High-energy synchrotron x-ray scattering experiment

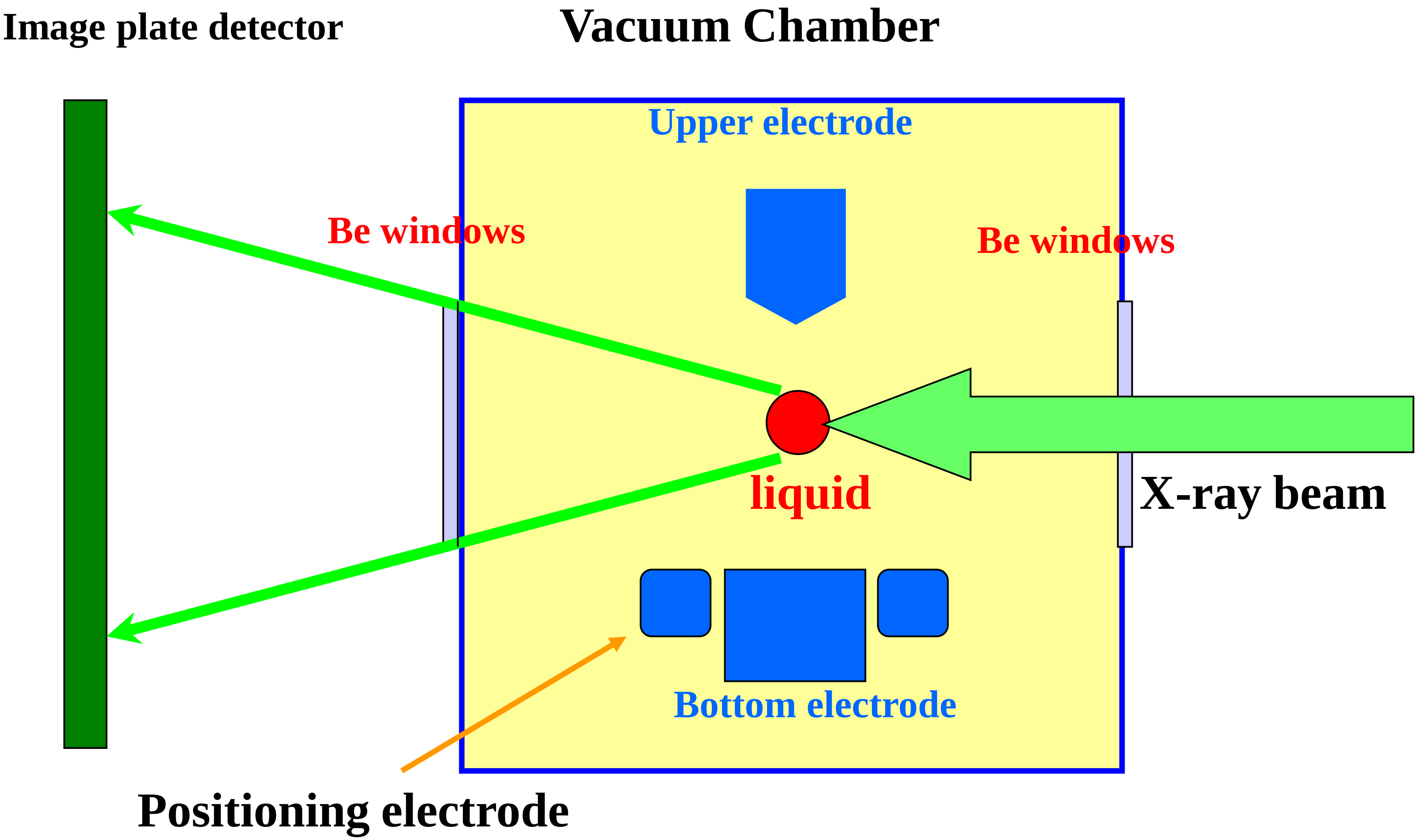

Sample size : 30-100 mg,
Temperature : 300-2200 K,

X-ray Energy : 125 keV,
Vacuum :10^{-7} torr

Wavelength : 0.0988 °A
Exposure time : 1 sec.


東亞日報

2009년 08월 07일 23면

인공우주장치로 '건담 합금'도 가능할까

"적 전차를 한 방에 꿰뚫는 강력한 탄환을 만든다. 노트북이나 휴대전화의 배터리 사용시간을 수십 배 늘린다."
지구에 자연적으로 존재하는 물질로는 이런 소재를 개발하기 어렵다.
지금보다 몇 배나 단단한 초금속.
전기저장량을 30배나 높인 물질이 있어야 하기 때문이다.
과학자들이 대신 찾은 곳은 우주 공간이다.
정확히 말하면 진짜 우주를 본뜬 '인공 우주'다.

1979년 소개된 만화영화 '기동전사 건담'의 주인공 로봇 'RX-78-2'. 이 로봇은 달에서만 제련할 수 있는 특수합금 '루나티타늄'으로 만든다. 동아일보 자료 사진

● 국내 첫 인공우주실험실

국내에서 첫 인공우주실험실이 등장했다. 한국표준과학연구원 이근우 연구원은 2년간 4억 원을 들여 인공우주를 구현한 '정전기식 공중부양장치'를 국내 최초로 개발했다. 우주공간과 비슷하게 '진공과 무중력의 공간'을 만드는 장치다. 세계에서는 8번째로 개발됐다.

진공을 만드는 것은 어렵지 않다. 펌프로 공기를 뽑아내면 된다. 그럼 어떻게 중력을 없앨까. 이 장치는 지구의 중력과 똑같은 힘을 내는 전기장을 중력 반대 방향으로 걸어준다. 중력과 전기장이 상쇄되면서 장치 안에 물체를 놓으면 우주인처럼 공중에 붕 떠오른다. 50mg의 시료라면 0.00005N(뉴턴)의 전기적인 힘을 위로 쏴준다. 이 장치는 고출력 레이저로 공중에 뜬 물질을 섭씨 4000도까지 가열할 수도 있다. 이근우 연구원은 "장치를 거의 완성했을 때 실험용 물체가 제자리에 떠 있지 않고 엉뚱한 곳으로 튀어나가거나 마구 날아다녀 고생했다"며 "물체에 실을 매달고 한 달 동안 미세하게 조정한 끝에 장치를 완성했다"고 말했다.

로켓용 신소재를 연구하고 있는 한국항공우주연구원 이호성 책임연구원은 "중력은 재료과학 연구자들에게 가장 큰 걸림돌"이라며 이 장치를 반겼다. 중력이 있는 지구에선 실험물질을 꼭 어딘가에 '올려' 두어야 하며, 액체는 용기에 담아야 한다. 다른 물질이 닿아 있으니 당연히 실험결과에 오차가 생긴다. 녹는점이 섭씨 3033도에 달하는 오스뮴(Os) 같은 물질은 담아둘 용기조차 없다. 연구팀이 개발한 공중부양장치는 이런 한계를 극복해 '꿈의 실험'을 가능하게 한다. 주로 우주연구기관이 이 장치를 사용할 것으로 전망된다.

세계 8번째 '진공-무중력 공간' 구현
우주와 환경 유사해 각종 실험 가능

안깨지는 금속-저장량 늘린 배터리 등
'만화영화 같은' 신소재 개발 기대

● '메이드 인 스페이스' 신소재

1979년 처음 방영된 일본 애니메이션 '기동전사 건담'의 주인공 로봇은 달에서만 제련할 수 있는 '루나티타늄'이라는 금속으로 만든다는 설정을 갖고 있다. 대포보다 큰 120mm 포탄을 맞아도 끄떡없고, 고열이나 방사능도 차단한다. 우주에서는 지구보다 더 뛰어난 소재를 만들 수 있을 거라는 상상력이 만들어 낸 가상의 물질이다. 과학자들은 인공우주실험실에서도 '만화영화 같은' 신소재를 만들 수 있을 거라고 기대한다.

미국항공우주국(NASA)은 1992년 인공우주실험실에서 '비결정질 금속'이라는 신소재를 개발했다. 금속이 깨지는 이유는 물질이 결정 형태로 굳어 있기 때문인데 비결정 금속은 결정을 이루지 않아 잘 깨지지 않는다. 이 기술은 현재 전차의 장갑판, 대포알의 탄두, 고탄력 테니스 라켓 등 다양한 첨단물질을 만드는 데 응용되고 있다. 일본우주항공연구개발기구(JAXA) 연구진도 2006년 비슷한 실험장치를 이용해 전기저장량을 30배나 늘린 배터리용 신물질을 개발했다.

아무리 인공 우주라도 진짜 우주만 할 수는 없다. 그래서 국제우주정거장(ISS)을 거대한 우주실험실로 활용하는 방법도 모색되고 있다. NASA는 이미 우주정거장에 소재 개발을 위한 실험장치를 운영하고 있으며 일본도 곧 비슷한 장치를 설치할 예정이다. 이근우 연구원은 "처음에는 국내에 이 장치를 아는 사람이 없어 일부에선 '쓸모없는 일을 한다'는 냉소도 많았다"며 "앞으로 이 장치를 활용해 나노미터 크기의 초미세 반도체 소자를 연구할 계획"이라고 말했다.

대전=전승민 동아사이언스 기자 enhanced@donga.com

공중부양장치는 전기장을 이용해 물체를 공중에 띄울 수 있다. 알루미늄 금속이 떠 있는 모습. 사진 제공 한국표준과학연구원

(25.7×27.8)cm

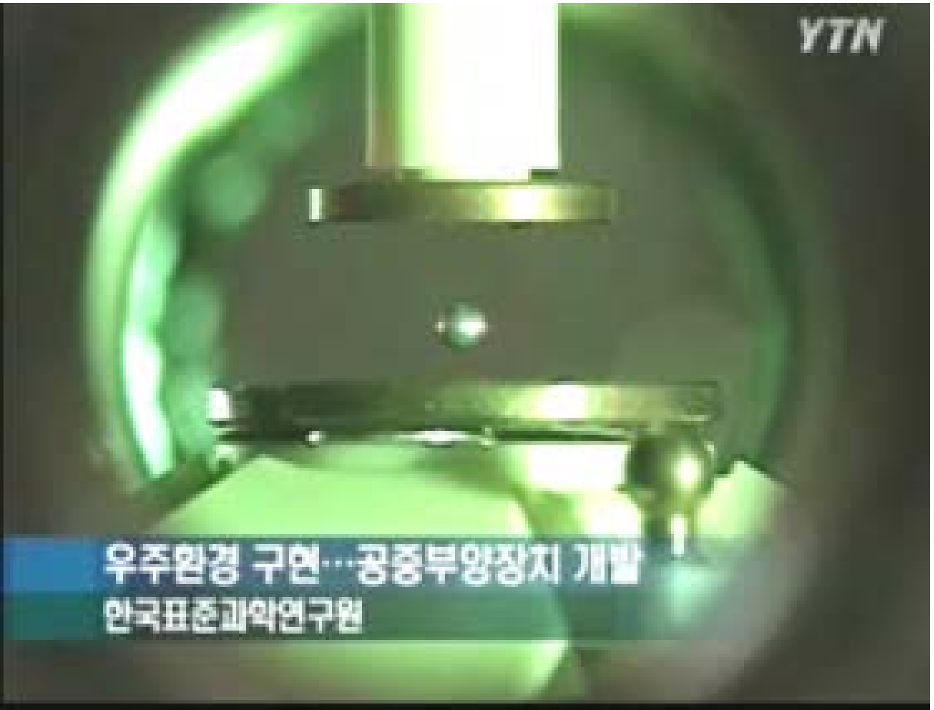

Electrostatic Levitation in KRISS

Containerless equipment: close to homogeneous nucleation

T: ~3000 °C
P: ~ 10^{-7} Torr

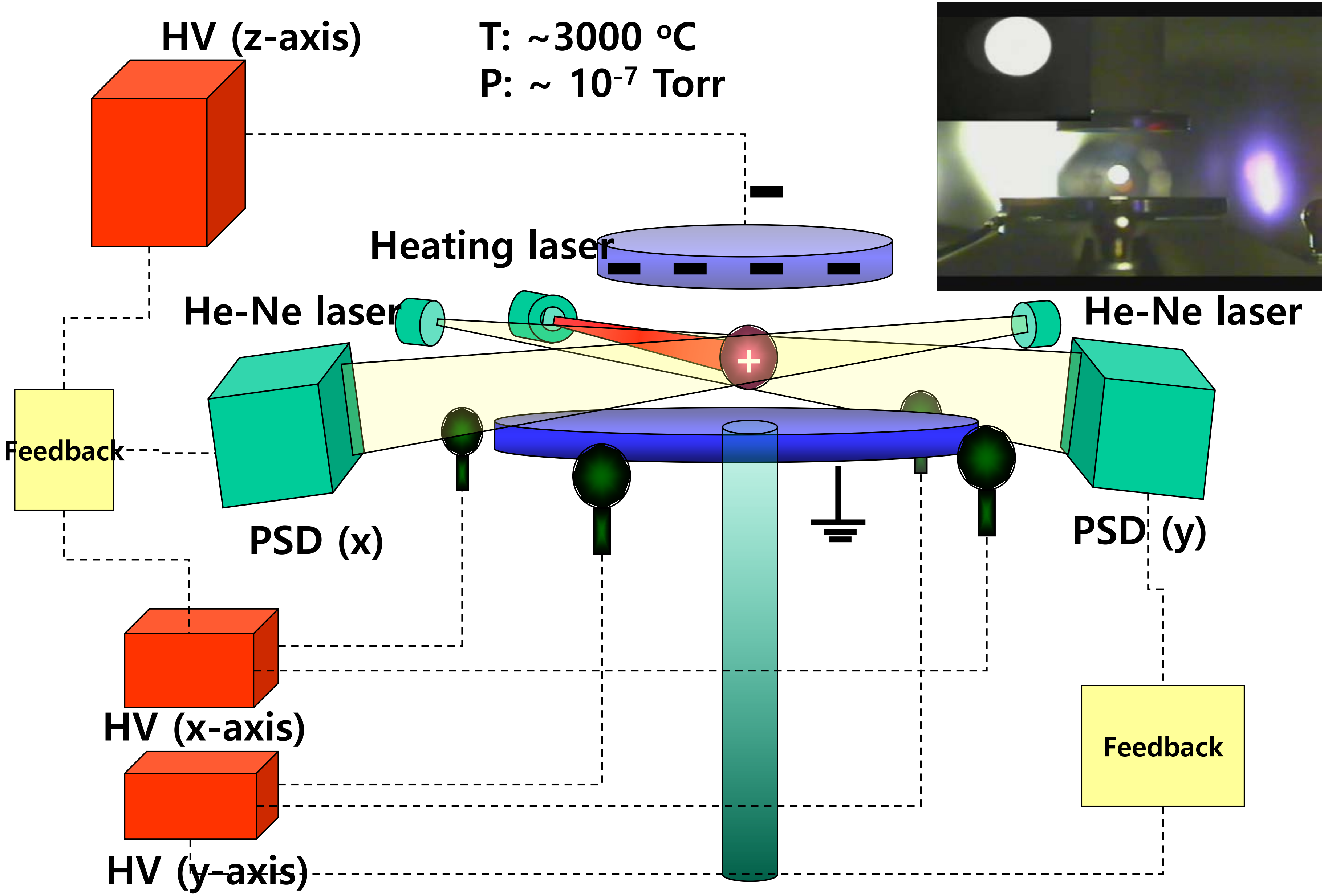

- No solid containers, No impurities from container
  - No heterogeneous nucleation site
    - Extremely large supercooling can be obtained, clear recalescence
      - Metallic glass can be formed through free cooling

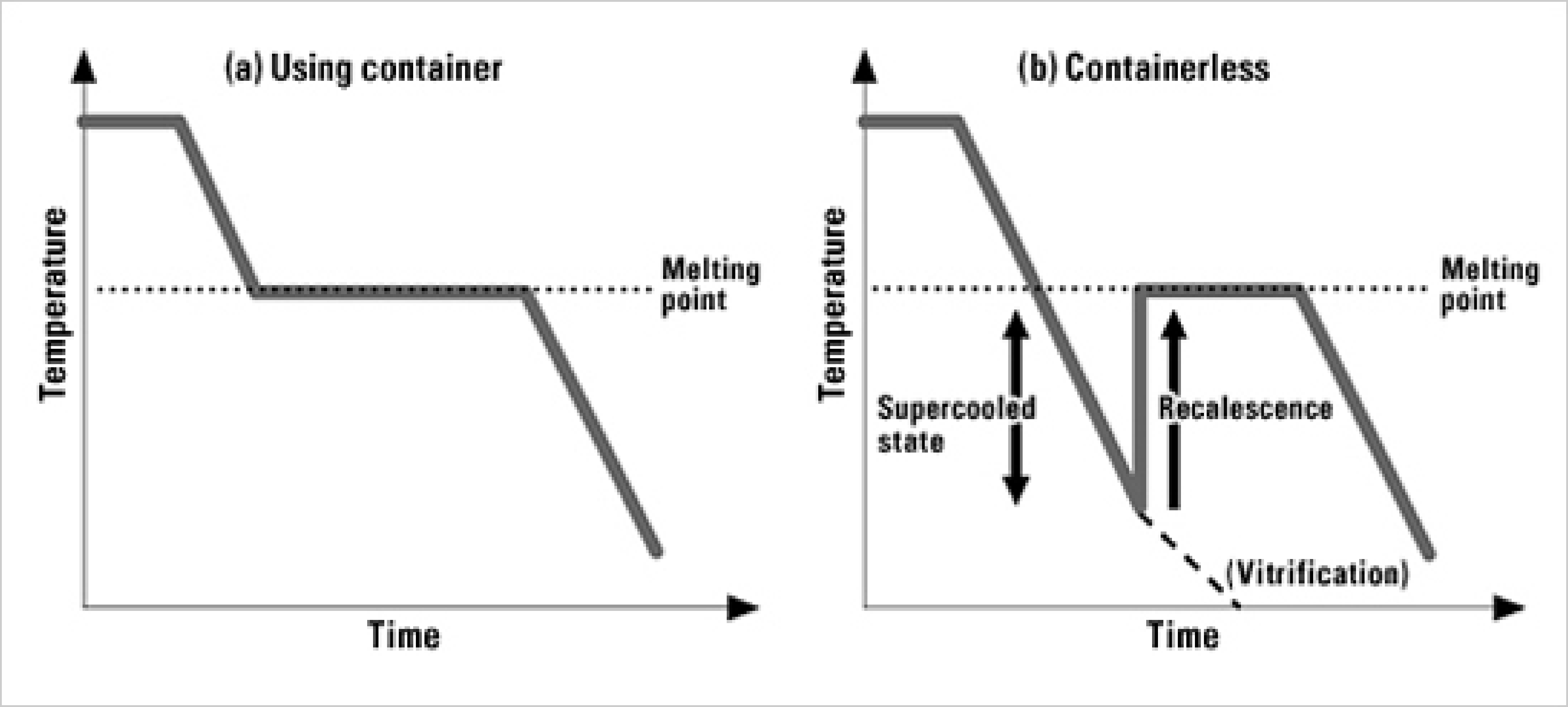

1) Melting and Freezing Using ESL

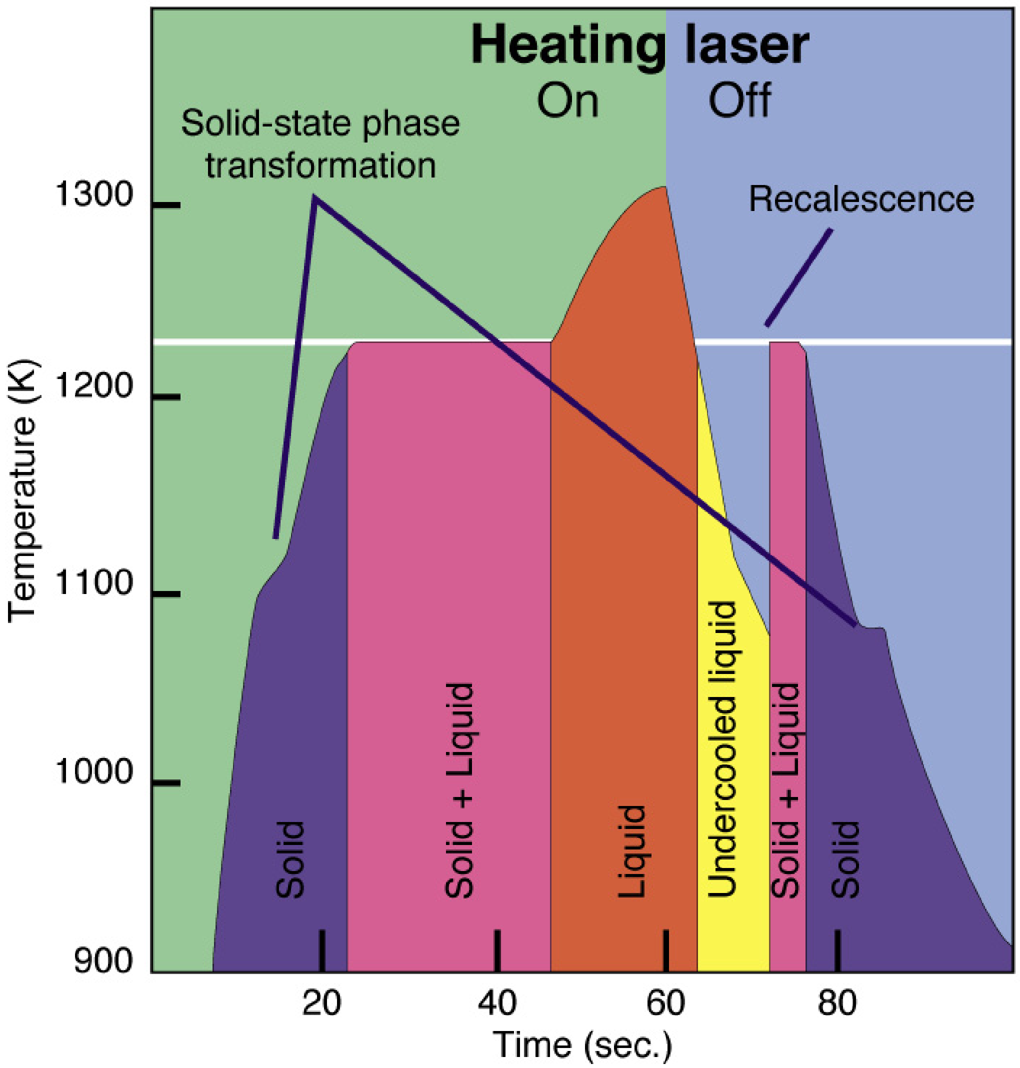

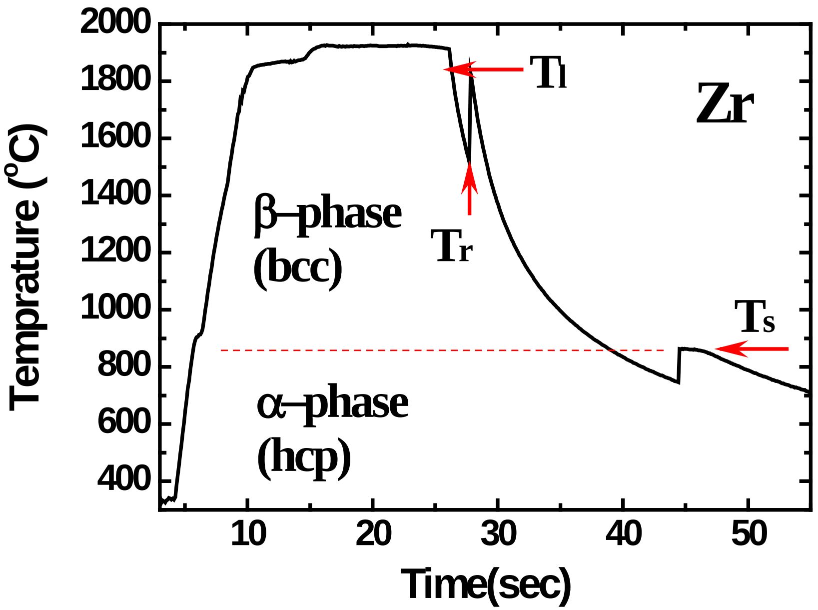

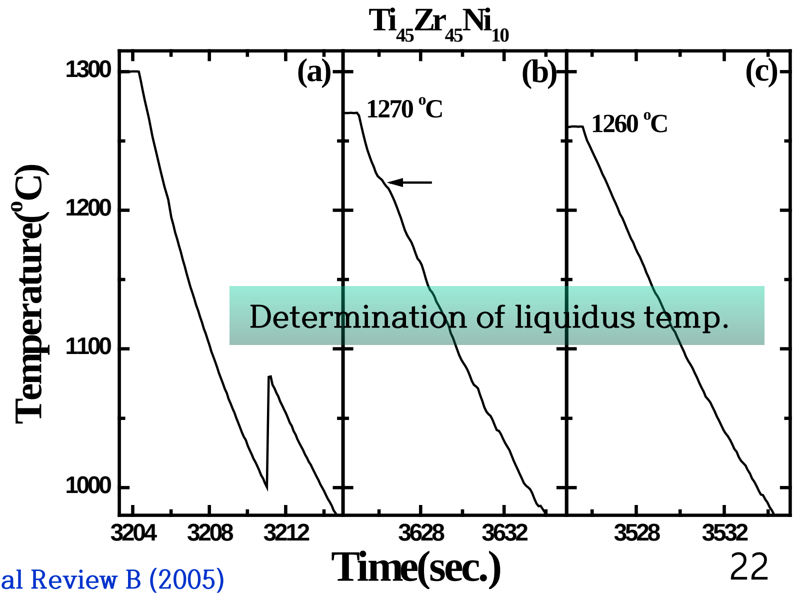

Determination of liquidus temp.

Lee, Gangopadhyay, Kelton, et.al., Physical Review B (2005)

Cyclic cooling curves of $Zr_{41.2}Ti_{13.8}Cu_{12.5}Ni_{10}Be_{22.5}$

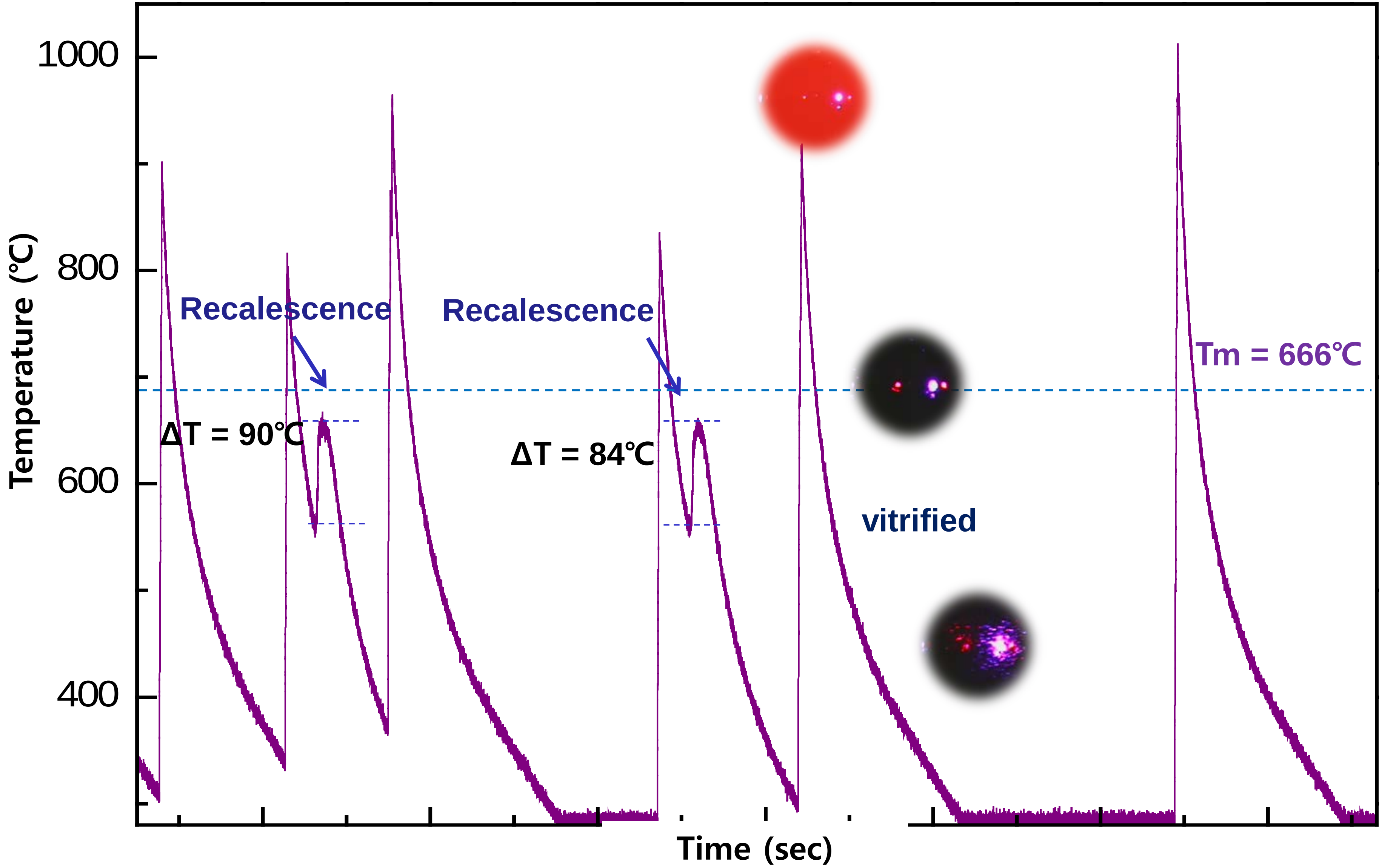

3) Measurement of TTT diagram _ $Zr_{41.2}Ti_{13.8}Cu_{12.5}Ni_{10}Be_{22.5}$

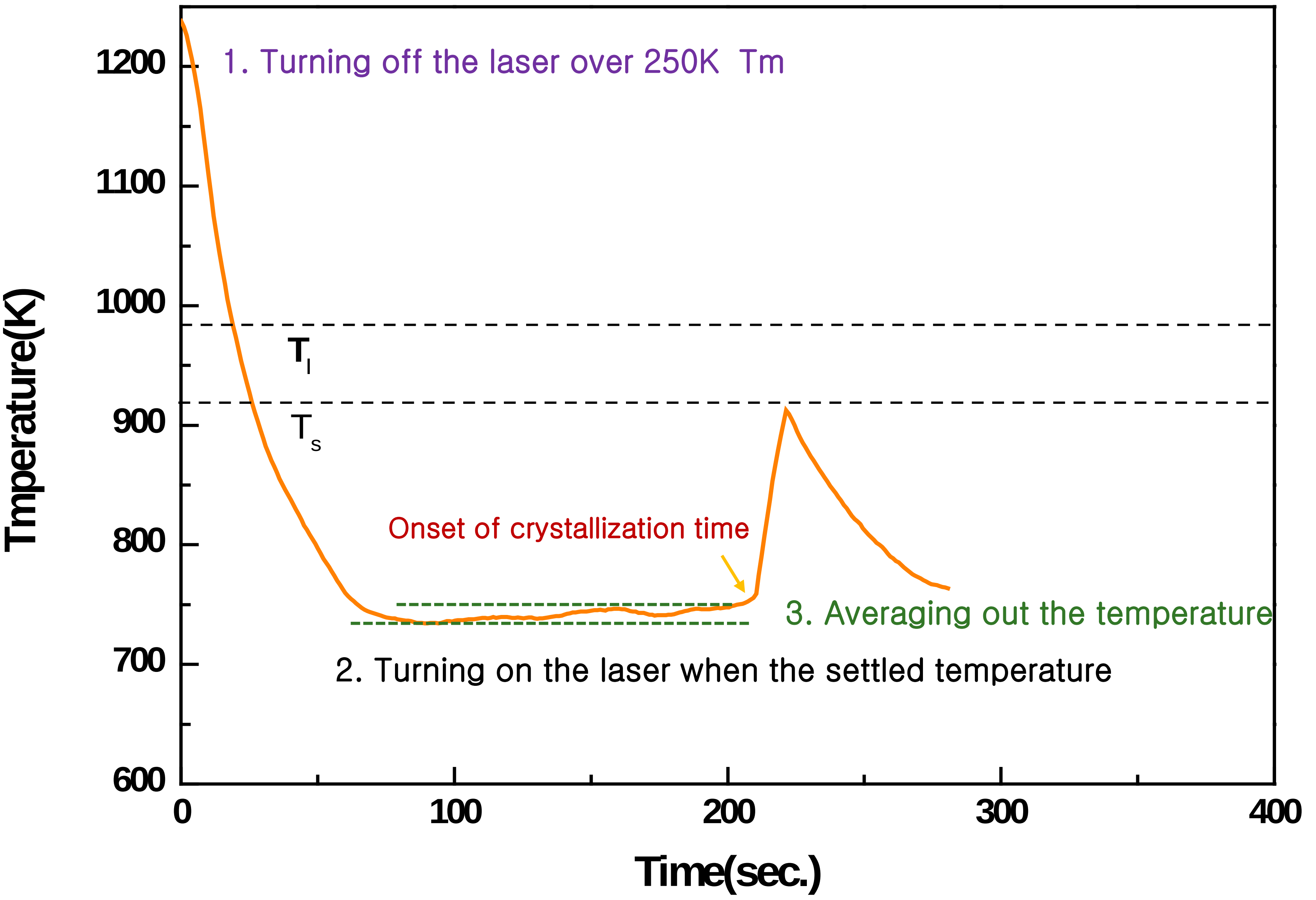

1. Turning off the laser over 250K Tm

Onset of crystallization time

3. Averaging out the temperature

2. Turning on the laser when the settled temperature

Measurement of TTT diagram _ $Zr_{41.2}Ti_{13.8}Cu_{12.5}Ni_{10}Be_{22.5}$

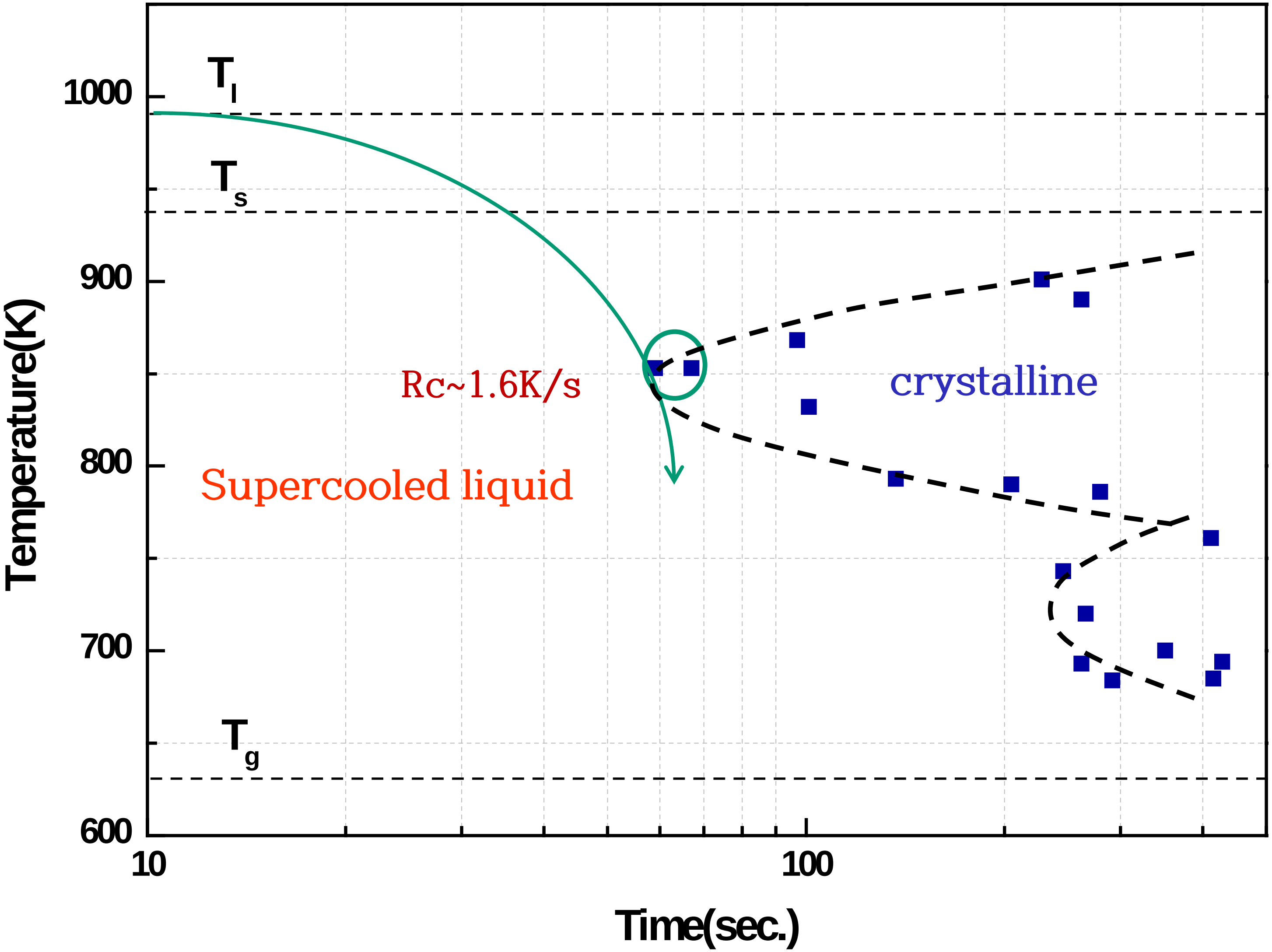

4) Specific heat capacity

ε=0.24, 0.24, 0.19

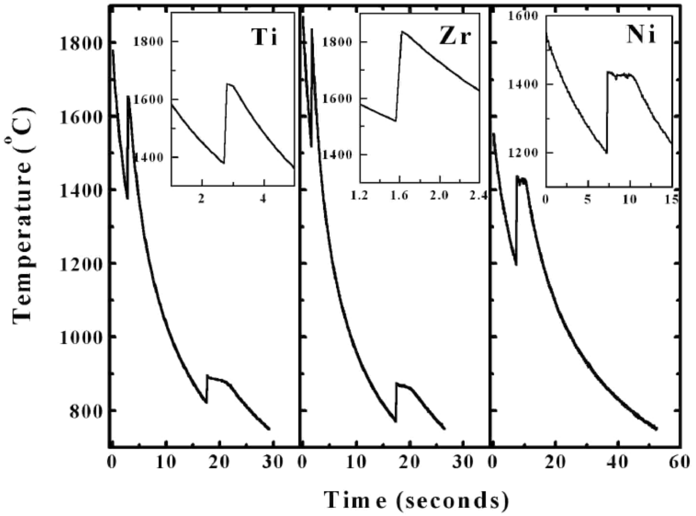

Figure 6.1. Free cooling curves of Ti, Zr and Ni, measured in the ESL. Inset figures show recalescences at high temperature.

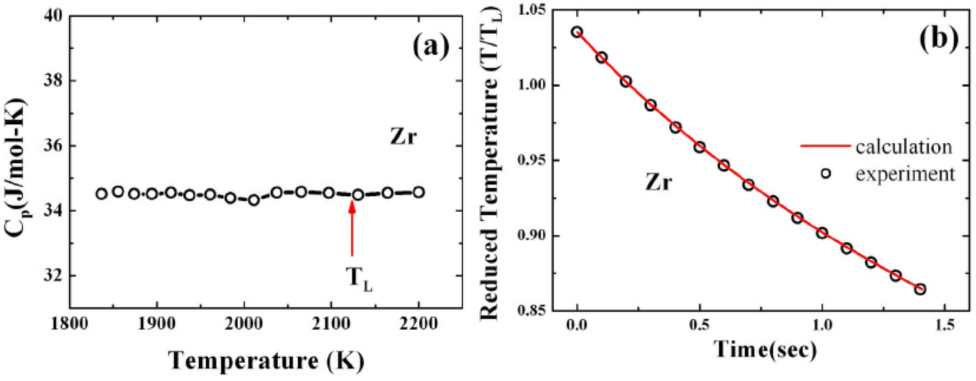

$$t = \frac{mC_p}{4\sigma\varepsilon A T_r^3}\left(\ln\left(\frac{(T+T_r)(T_i-T_r)}{(T-T_r)(T_i+T_r)}\right) + 2\tan^{-1}\left(\frac{T}{T_r}\right) - 2\tan^{-1}\left(\frac{T_i}{T_r}\right)\right)$$

$$\boxed{mC_p\left(\frac{dT}{dt}\right) = 4\pi r^2\sigma\varepsilon\left(T^4 - T_s^4\right)}$$

Specific heat of pure elements

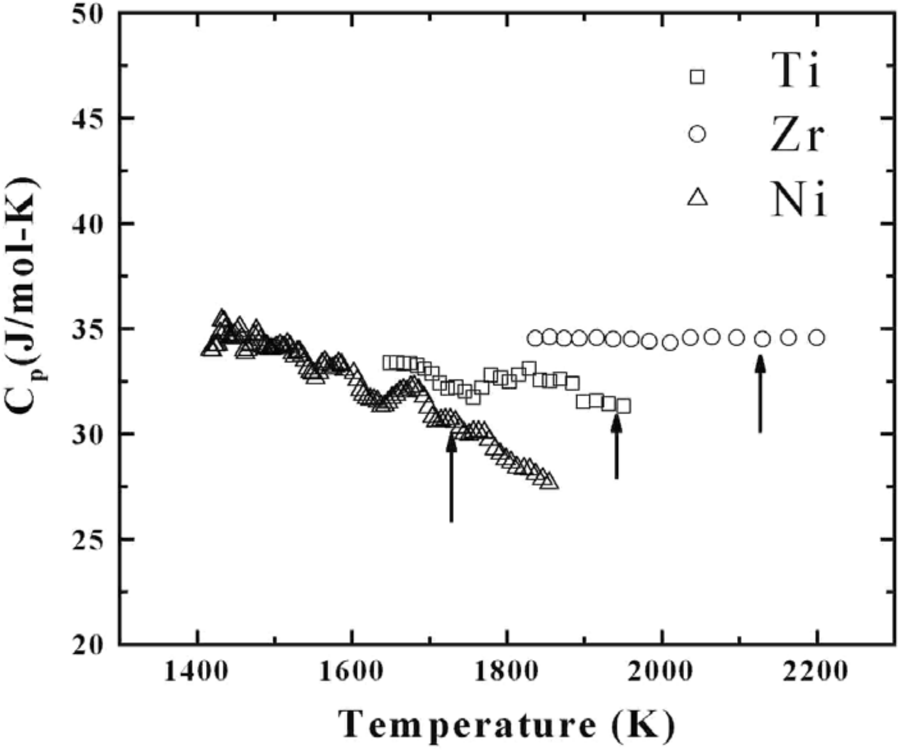

5) Emissivity

$$mC_p\left(\frac{dT}{dt}\right) + Power = 4\pi\sigma\varepsilon\left(T^4 - T_o^4\right)$$

$$Steady \quad condition, \quad \left(\frac{dT}{dt}\right) = 0$$

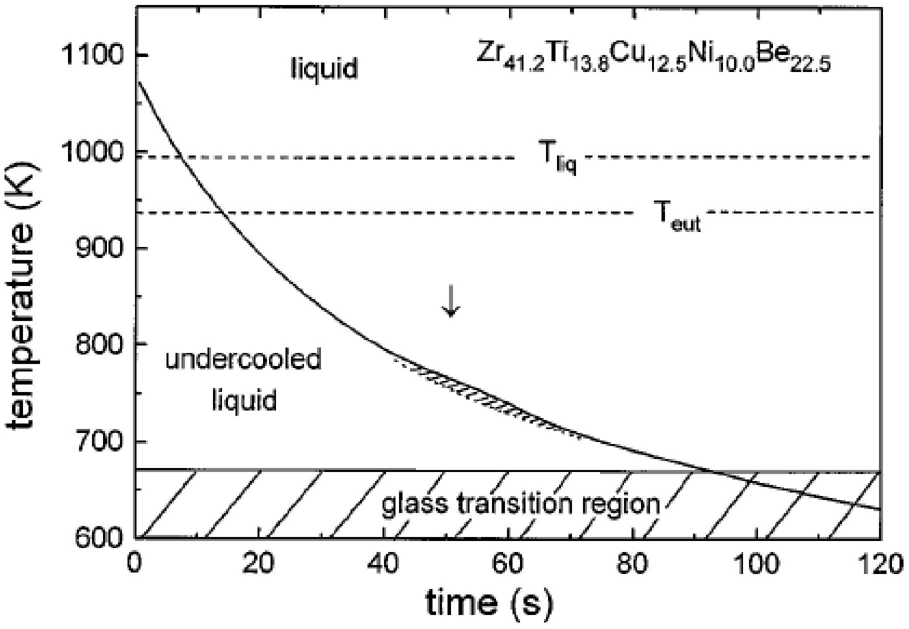

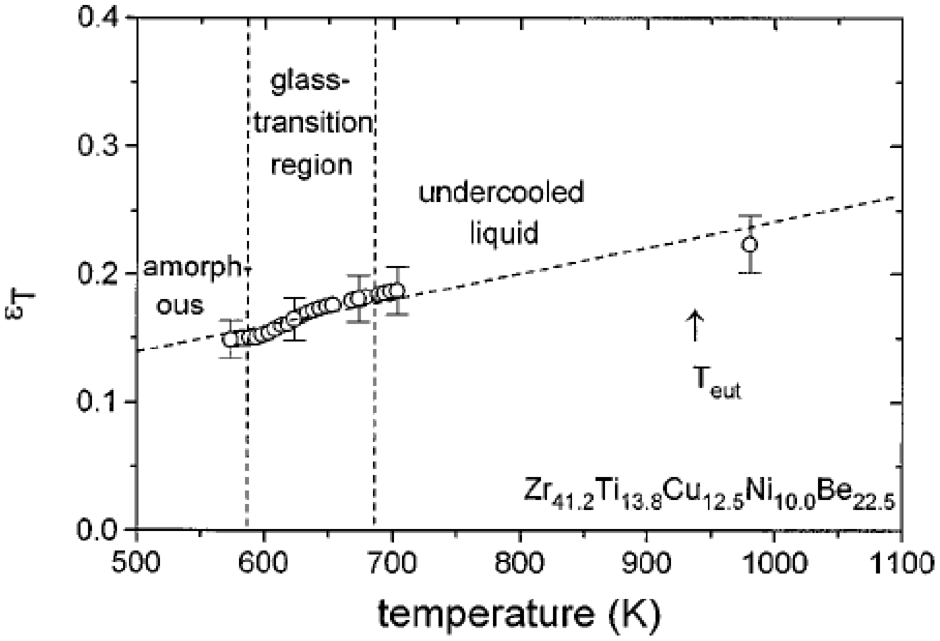

Kim, et.al., APL v68 (1995)

6) Fusion Enthalpy

$$\Delta H_f = (1) + (2) = C_p \Delta T_r + (4\pi\sigma\varepsilon(T_P{}^4 - T_o^4)\Delta t - 4\pi\sigma\varepsilon(T_P{}^4 - T_{end}^4)\Delta t)$$

Crystallization

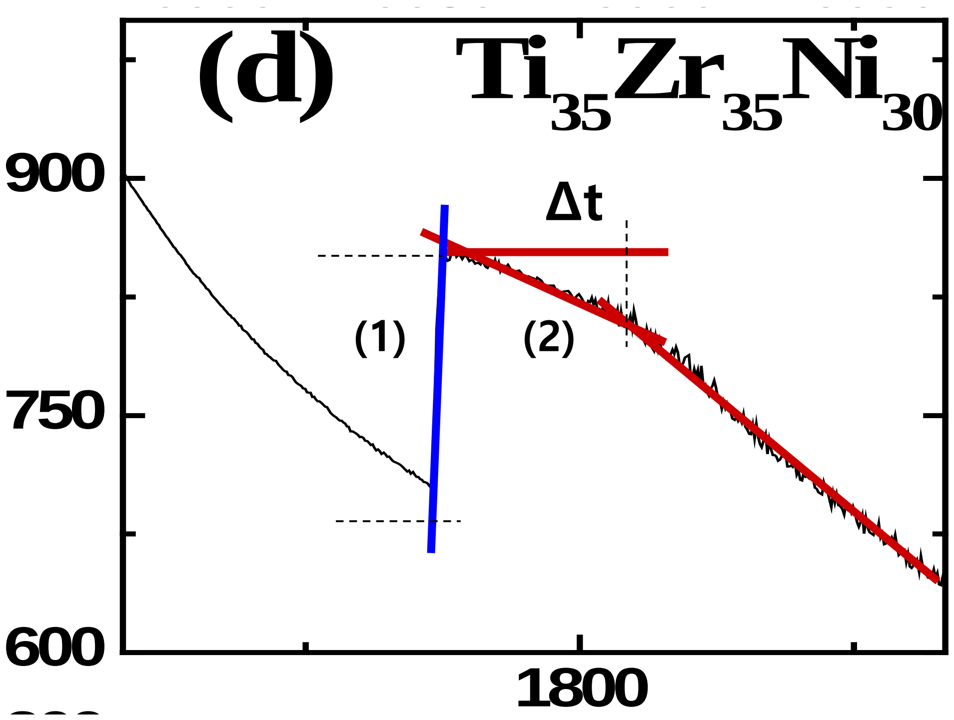

이근우: gwlee@kriss.re.kr

7) Viscosity & Surface Tension: Oscillation

Snapshot of surface oscillations in a Ni droplet

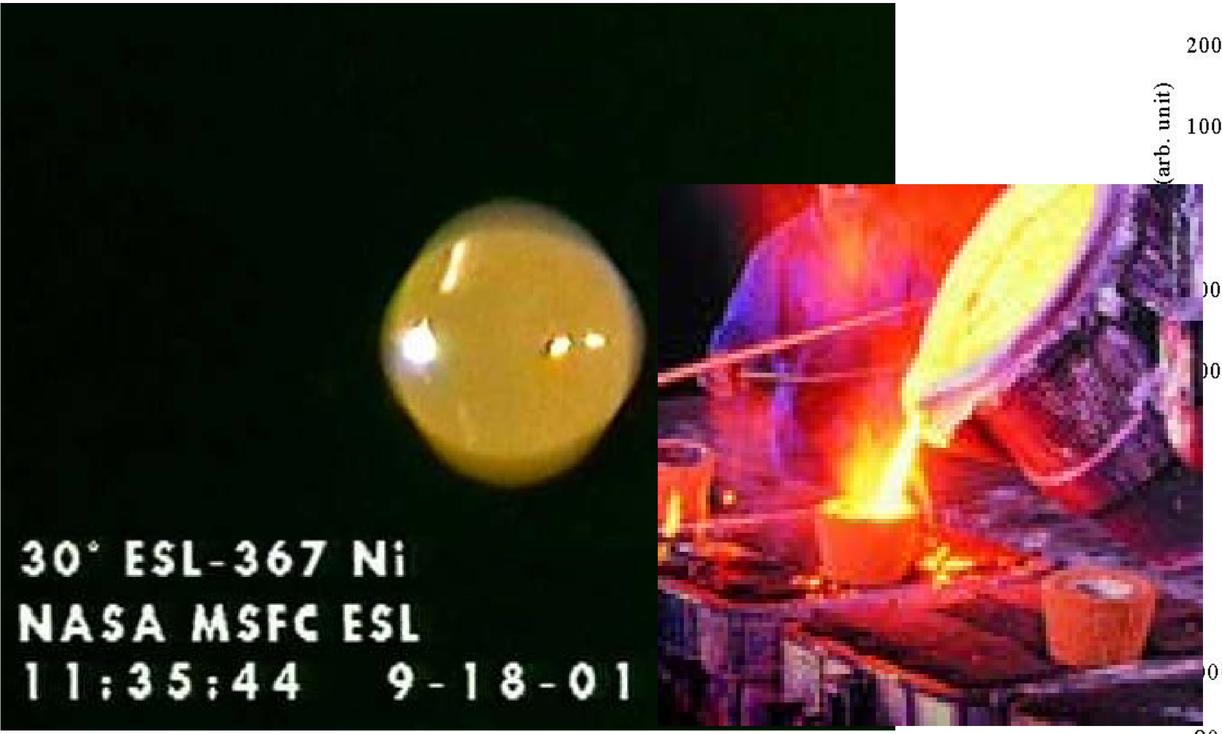

Damped oscillations

Exponential decay of amplitude

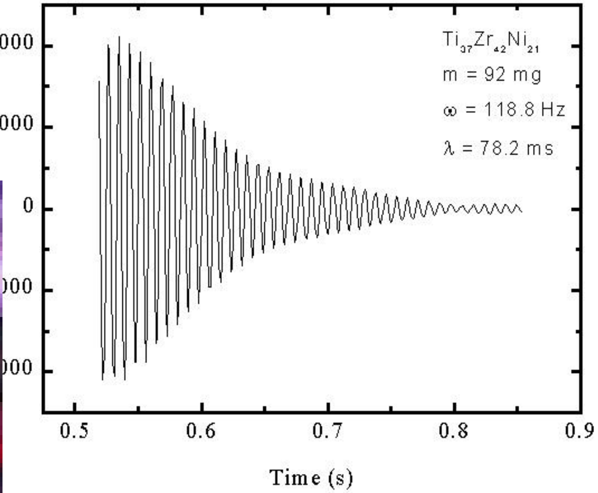

Power Spectrum

Single frequency

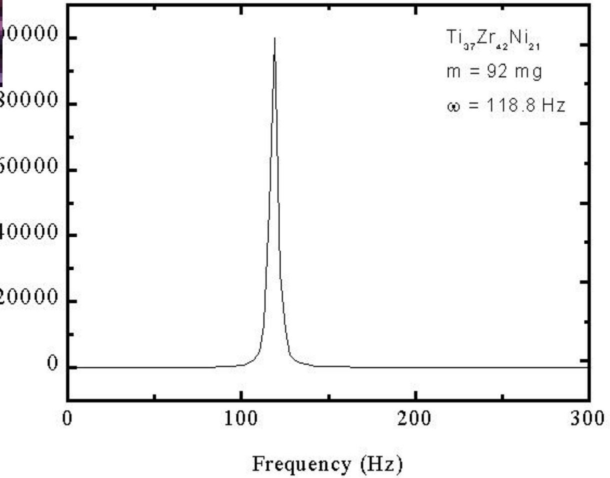

Caution: No distortion from spherical symmetry allowed multiple modes will be excited

Measurement of thermophysical properties

- Volume : CCD camera / Temperature measurement : pyrometer

- Surface tension & Viscosity : oscillating the sample by with a pulse of AC voltage

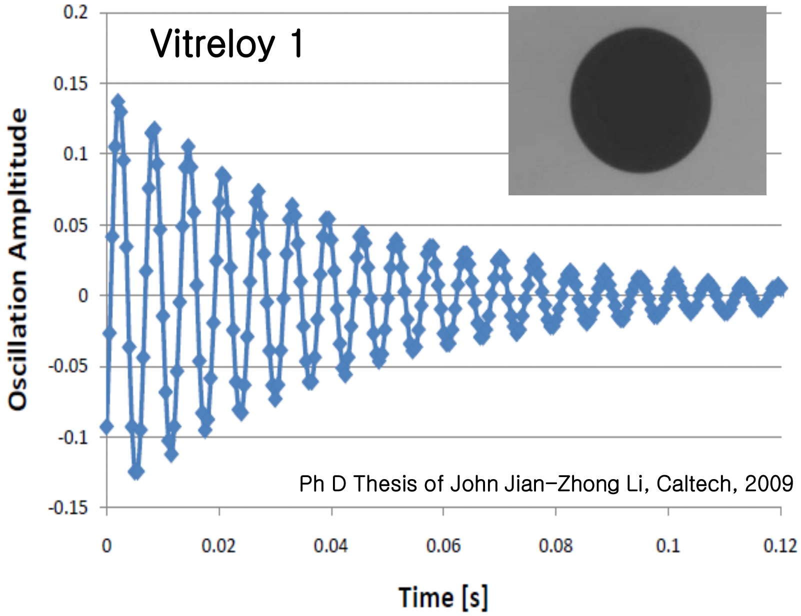

Ph D Thesis of John Jian-Zhong Li, Caltech, 2009

$$\omega_2^2 = \frac{8\gamma}{\rho r_0^3}$$

Oscillation frequency

Surface tension

Radius
when melt adopts
a spherical shape

Density

$$\frac{1}{\tau_2} = \frac{5\eta}{\rho r_0^2}$$

Decay time
constant

Viscosity

- Specific heat & total hemispherical emissivity : $\frac{m}{M} C_P \frac{dT}{dt} = -\sigma_{SB}\varepsilon_T A(T^4 - T_S^4)$

- Time- temperature-transformation curve : isothermal treatment

Oscillating drop 방식으로 고온에서 metal의 점도/ 표면 장력 측정 가능

Oscillating drop

- Induce surface oscillations in a levitating liquid droplet of radius ‘R_o’, mass ‘m’
- Measure the frequency of oscillation (ω)
- Measure the damping constant (λ)

- Damped resonant oscillations:

$$R = R_0(1 + \delta \cos(\omega t) e^{-\lambda t})$$

Rayleigh (1879)

- Resonant frequency determined by surface tension:

$$\omega_l = \sqrt{\frac{l(l-1)(l+2)\gamma}{\rho R_o^3}}$$

- Damping determined by viscosity:

$$\lambda_l = \frac{(l-1)(2l+1)\eta}{\rho R_o^2}$$

Lamb (1881)

a) High Temp. Viscosity

JOURNAL OF APPLIED PHYSICS 100, 103523 2006

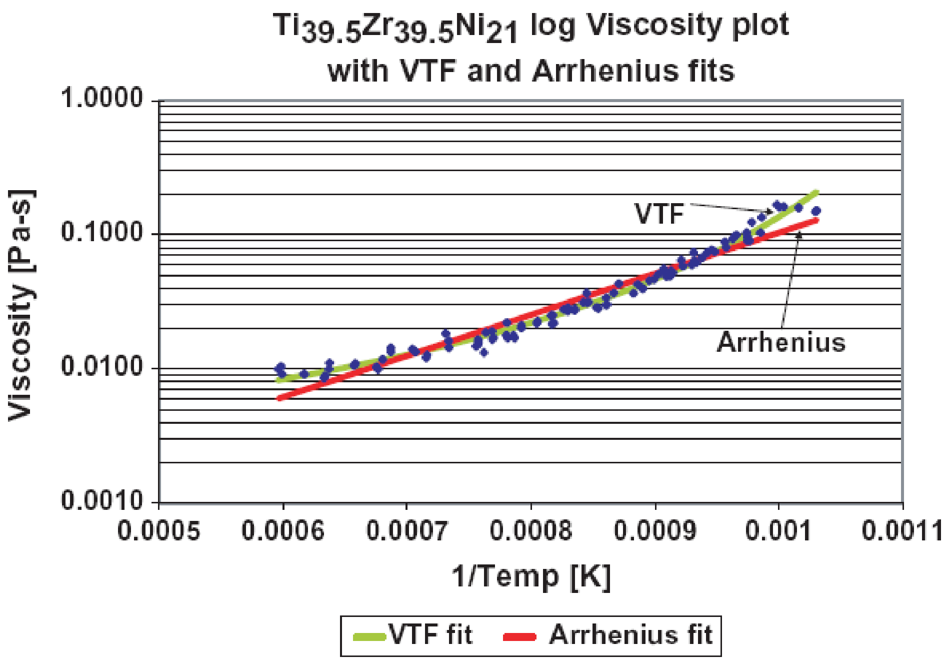

Hyers, et.al., Philosophical Magazine Vol. 86, 2006(341-347)

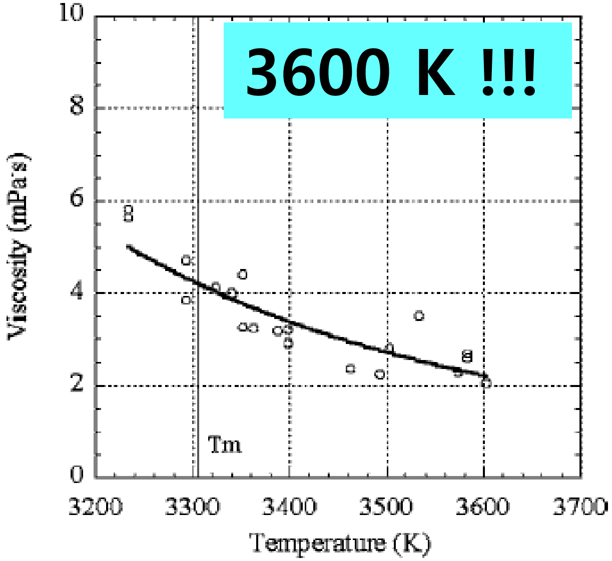

FIG. 5. Viscosity of equilibrium and nonequilibrium liquid Os as a function of te

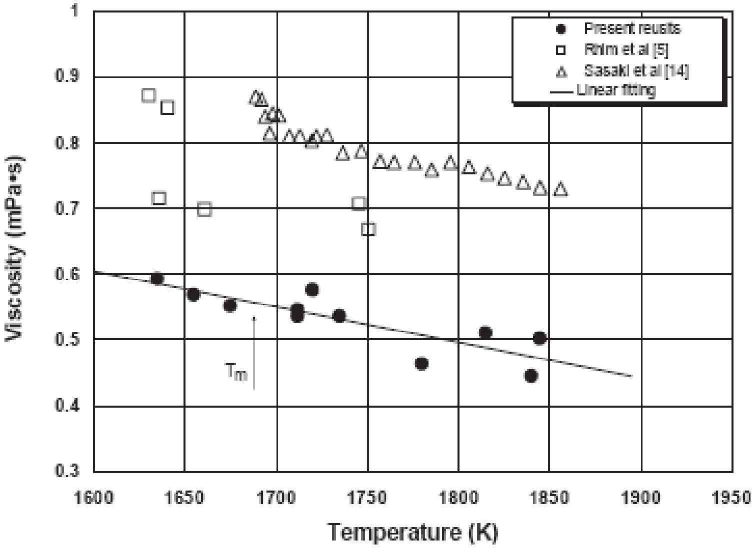

Fig. 8. Viscosity of molten silicon as a function of temperature.

b) High Temp. Surface Tension

Hyers, et.al., Philosophical Magazine Vol. 86, 2006(341–347)

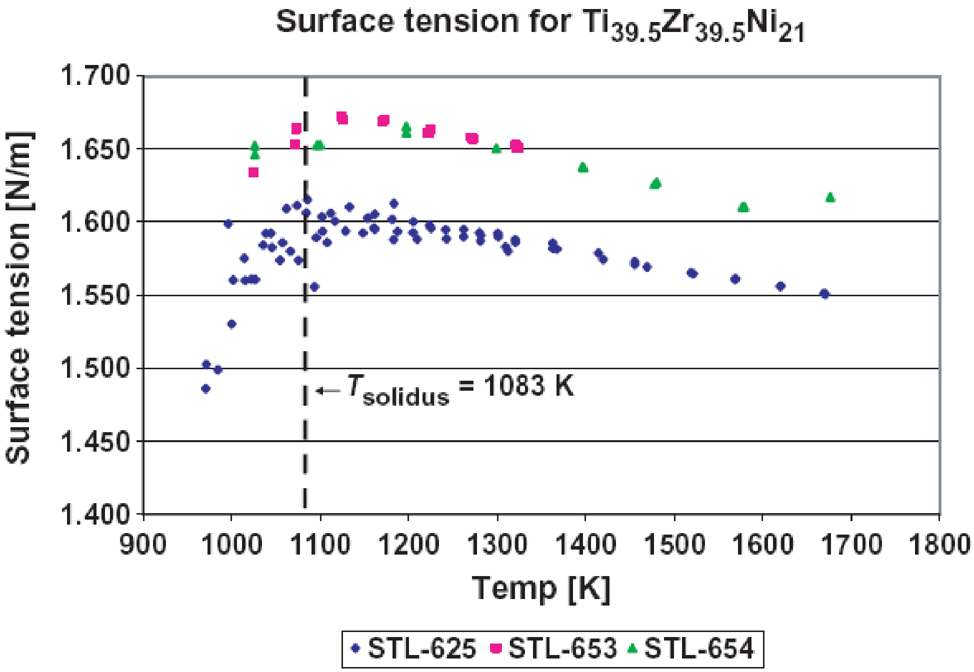

JOURNAL OF APPLIED PHYSICS 100, 103523 2006

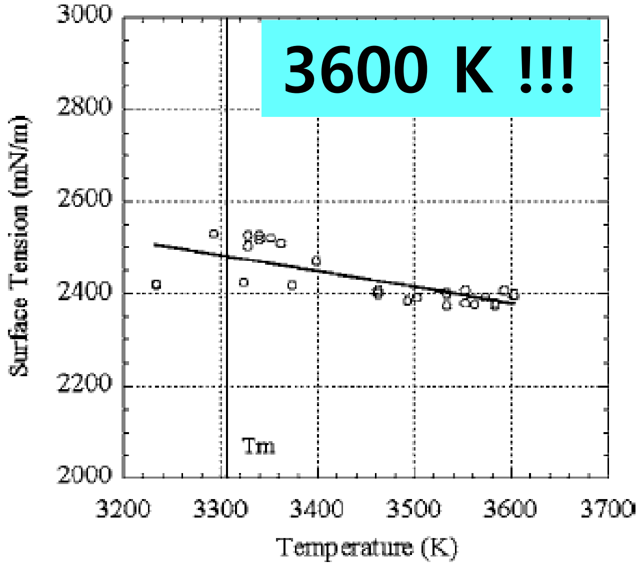

3600 K !!!

FIG. 4. Surface tension of equilibrium and nonequilibrium liquid Os as a function of temperature.

c) Density

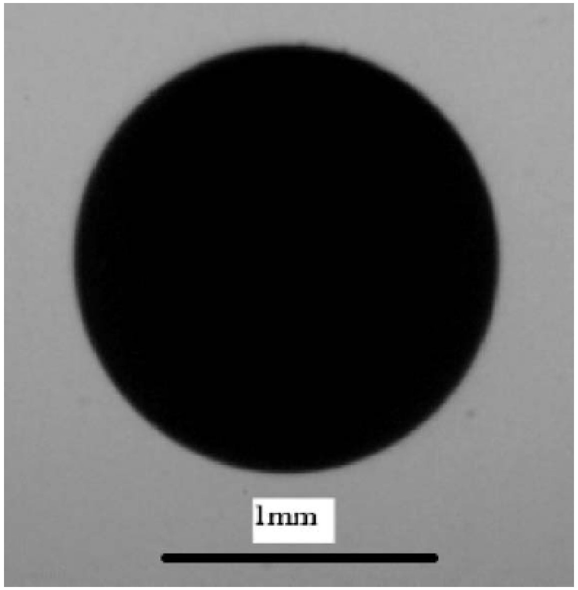

Fig. 2. A typical side view of a levitated molten silicon from which the density and the specific volume could be extracted.

Paradis, et.al., JOURNAL OF APPLIED PHYSICS 100, 103523 2006

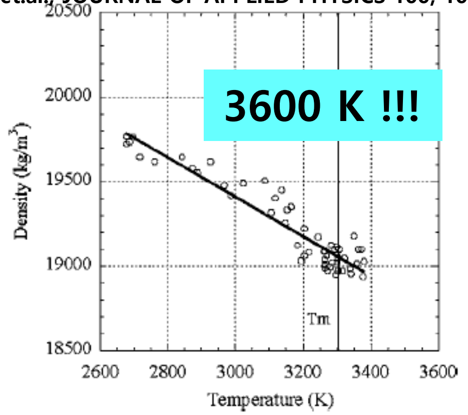

3600 K !!!

FIG. 3. Density of equilibrium and nonequilibrium liquid Os as a function of temperature.

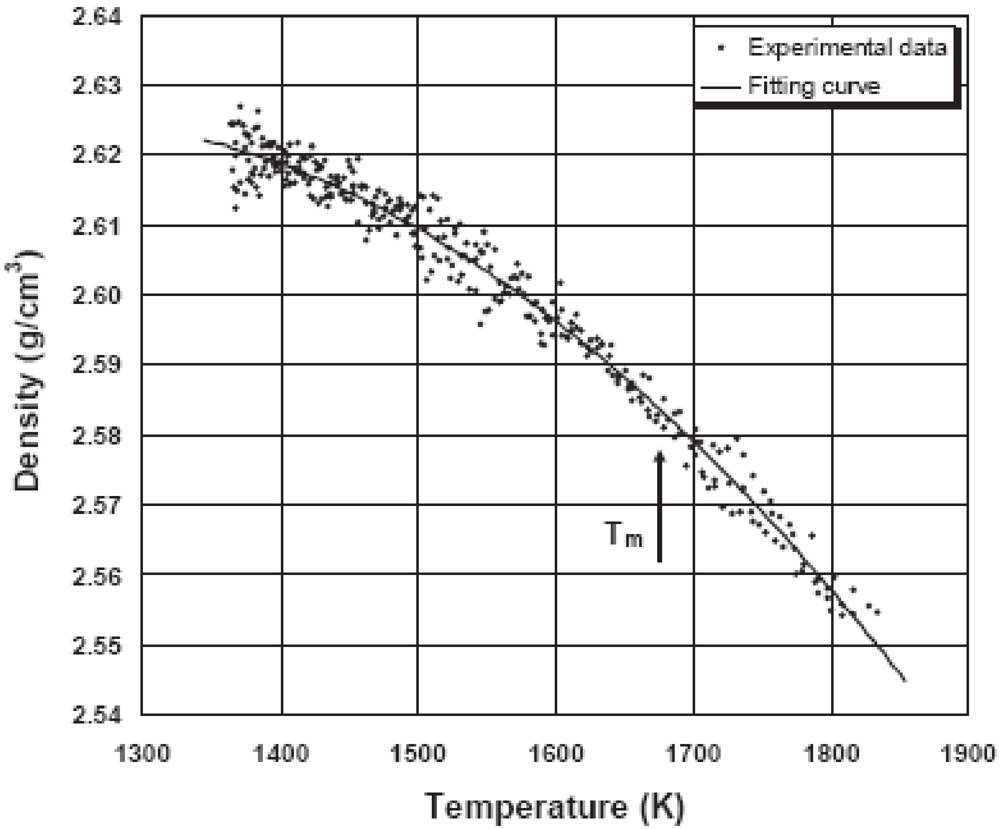

Fig. 4. Temperature dependent density of molten silicon.

Cooling curve and density temperature profiles of $Zr_{41.2}Ti_{13.8}Cu_{12.5}Ni_{10}Be_{22.5}$

- Volume : CCD camera / Temperature measurement : pyrometer

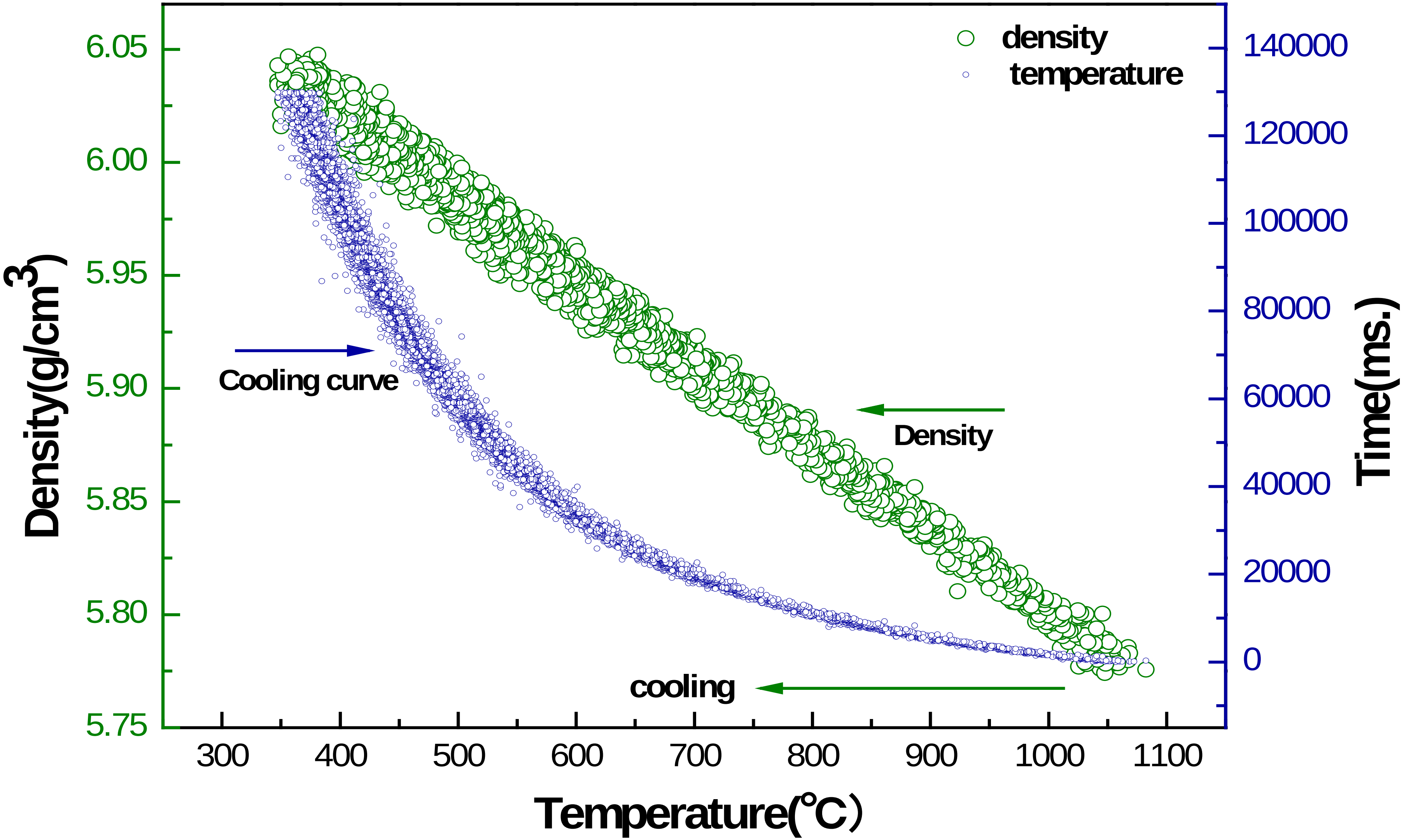

Crystallization: Undercooling of Os

Paradis, et.al., JOURNAL OF APPLIED PHYSICS 100, 103523 2006

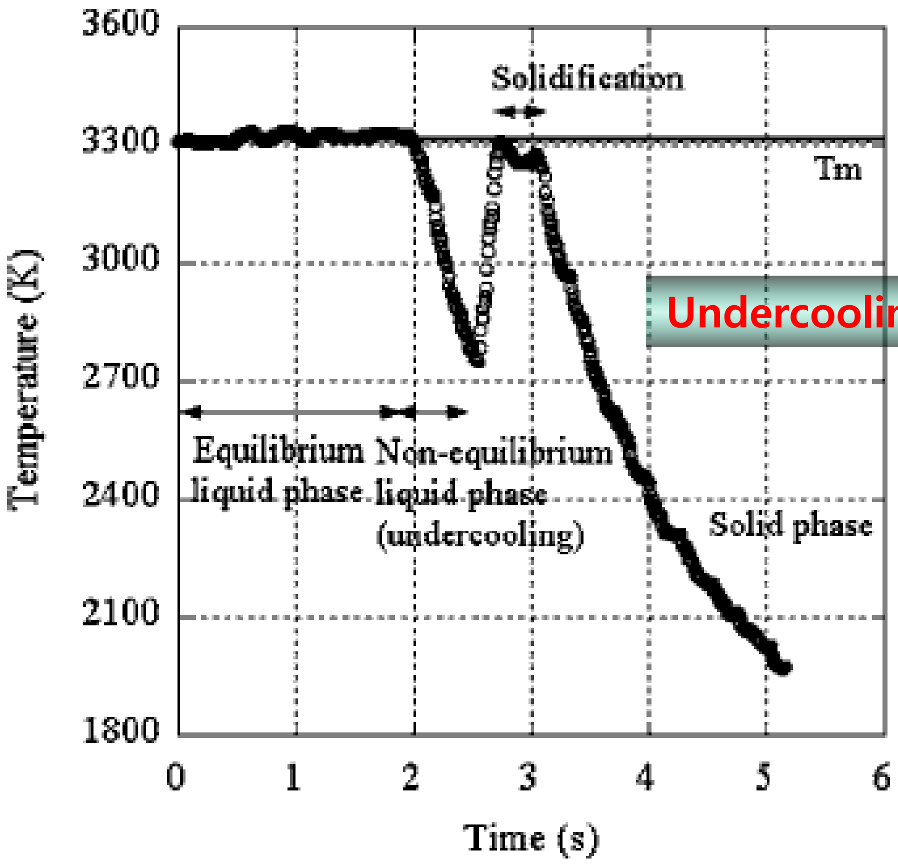

Undercooling:~575 K

FIG. 2. Temperature history for an Os sample (diameter: ~1.76 mm; mass: 64.18 mg) showing heating slightly above the melting temperature (~3340 K), a radiative cooling rate of 1015 K/s, an undercooling of ~575 K, recalescence, and solidification.

Interfacial free energy of some elements

	ΔT_r ΔT_{hyp} (K)	σ [1] (J/m²)	σ (J/m²)	$\alpha = \sigma / \Delta H_f$	r^* (nm)	ρ (g/cm³)	η_m [2] (10^{-3} Pa/s)	C_p (J/mol·K)	ΔH_f [3] (J/mol)
Ti	309 341	0.168	0.141 0.152	0.42 0.454	1.46 1.43	4.11	5.2	42.67	14550
Zr	332 345	0.158	0.154±0.009 0.159±0.010	0.410 0.423	1.54 1.52	6.08	4.67	42.5	19300
Hf	339 339	0.229	0.193±0.012	0.404	1.47	12.24	7.07	60.3	24070
Nb	443 563	0.262	0.258±0.016 0.303±0.024	0.394 0.462	1.33 1.23	7.63	4.94	52.0	29300
Rh	413 546	0.279	0.261±0.018 0.313±0.029	0.439 0.527	1.08 1.19	10.8	4.97	41.4	22600
Fe	195 357	0.269	0.158 0.228	0.33 0.478	1.45 1.15	[illegible]	[illegible]	[illegible]	[illegible]

- Turnbull : α = 0.45 for most metals

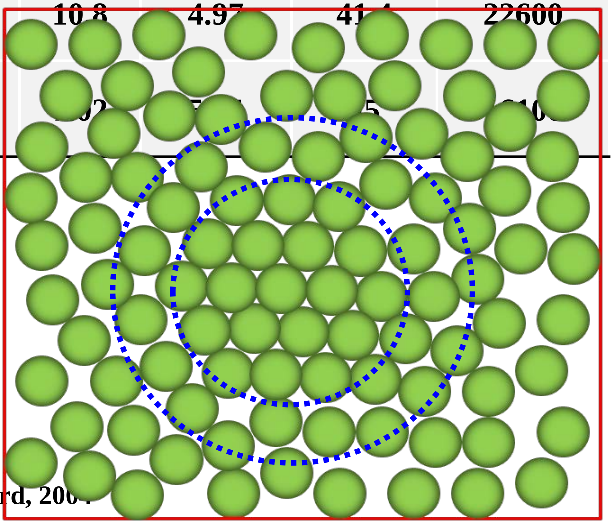

---

[1] B. Vinet, L. Magnusson, H. Fredriksson, P. J. Desré, *J. Colloid Interf. Sci.* 255 (2002) 363

[2] T. Ishikawa, P.-F. Paradis, J. T. Okada, Y. Watanabe, *Meas. Sci. Technol.* 23 (2012) 025305

[3] W. F. Gale, T. C. Totemeier, in "Smithells Metals Reference Book", 8th ed. Butterworth-Heinemann, Oxford, 200

Development of extreme condition endurance materials

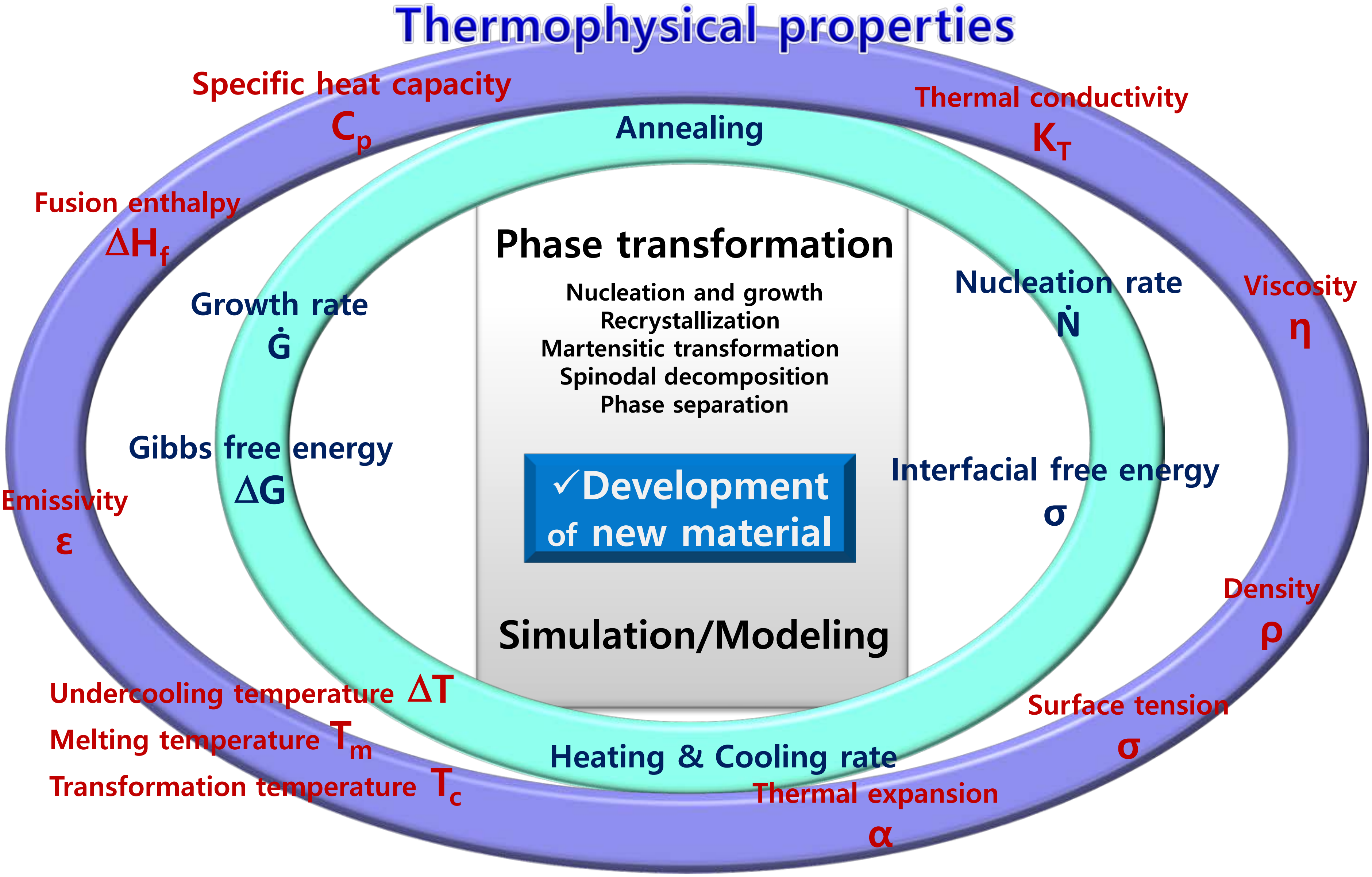

Thermophysical properties

Specific heat capacity C_p

Thermal conductivity K_T

Fusion enthalpy ΔH_f

Viscosity η

Emissivity ε

Density ρ

Surface tension σ

Thermal expansion α

Undercooling temperature ΔT

Melting temperature T_m

Transformation temperature T_c

Annealing

Growth rate $\dot{G}$

Gibbs free energy ΔG

Nucleation rate $\dot{N}$

Interfacial free energy σ

Heating & Cooling rate

Phase transformation

Nucleation and growth
Recrystallization
Martensitic transformation
Spinodal decomposition
Phase separation

✓Development of new material

Simulation/Modeling

3.2. Equilibrium condition for a curved interface

Stability of curved interface

1) Atomic consideration

a) Equilibrium: Geometrical factors $G_F = G_M$ (planer interface)

→ **If it is curved, “escape angle” changes with curvature.**

① S → L: if Solid is convex structure → G_M ↑, concave structure → G_M ↓

$\Delta G_M \propto$ curvature of the surface $\propto 1/r$

→ if “Spherical” crystal containing n atoms $\propto n^{1/3}$

② L → S: reverse direction of (S → L) case

∴ G_M^n for S → L transition

for atoms at the surface of a spherical crystal containing n atoms

$$G_M^n = (1 + \alpha / n^{1/3})\, G_M \quad , \; G_F^n = (1 - \alpha / n^{1/3})\, G_F$$

Convex surface = less firmly bound = fewer nearest neighbors in the crystal

→ easier escape than that of flat surface

b) Average energy for escape

$$L^{n} = (1 - \beta / n^{1/3})\, L_1$$

→ β is calculated from the number of neighbors

(ex. FCC structure: $\beta = 1.33$)

If the rate for the melting process ↑→ r ↓ &

the rate for the freezing process ↓→ T_E ↓.

$\therefore T_{E,\ \text{small crystal}} < T_{E,\ \text{large crystal}}$

Thus, at any temperature below T_E , there is a radius of curvature at which the rates of melting and of freezing are equal.

= critical radius r*

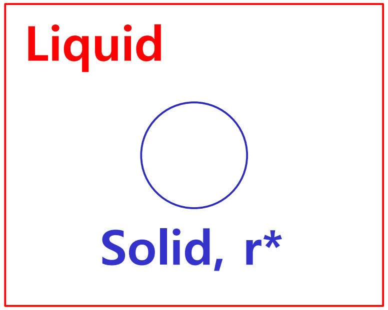

a) if $T_E + \Delta T\ (+)$, $R_M > R_F \rightarrow r \downarrow$

$\rightarrow T_E \rightarrow T_E{}' \downarrow \rightarrow \Delta T\ (+) \uparrow \rightarrow R_M >> R_F$

b) if $T_E + \Delta T\ (-)$, $R_M < R_F \rightarrow r \uparrow$

$\rightarrow T_E \rightarrow T_E{}'' \uparrow \rightarrow \Delta T\ (-) \uparrow \rightarrow R_M << R_F$

2) Thermodynamic treatment of equilibrium access a curved interface

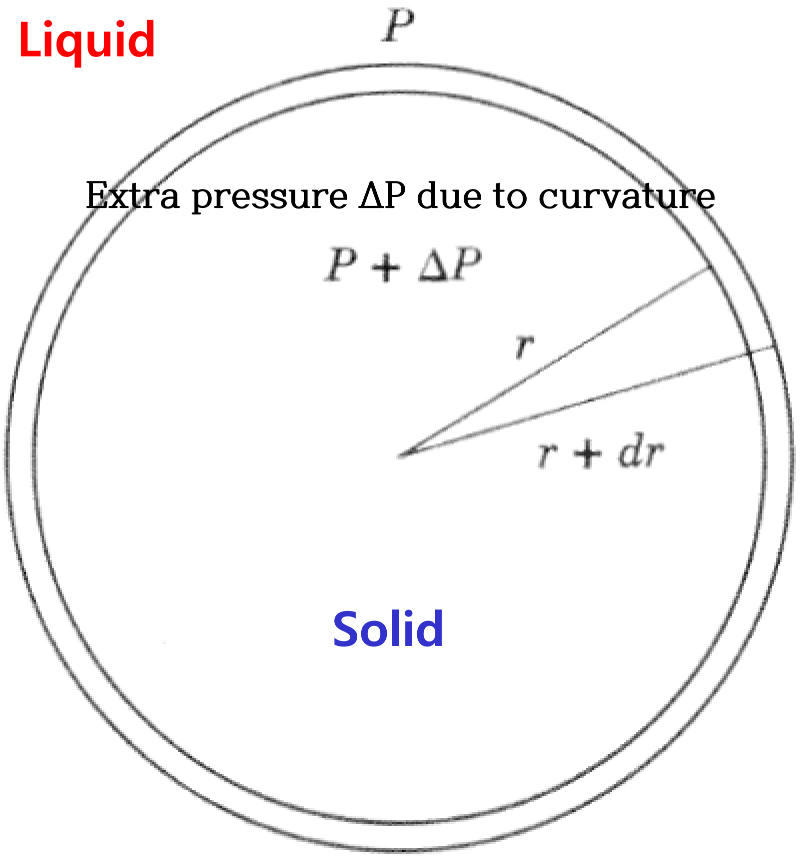

Fig. 3.1. Pressure due to surface tension.

$$r \to r + dr, \; P \to P + \Delta P$$

The work done is equal to the increase in free energy of the interface; Thus,

$$P\,dr \times 4\pi r^2 = [4\pi(r + dr)^2 - 4\pi r^2]\sigma$$

whence

$$\boxed{P = \frac{2\sigma}{r}}$$

The G curves so far have been based on the molar Gs of infinitely large amounts of material of a perfect single crystal. Surfaces, GBs and interphase interfaces have been ignored.

1.6 Influence of Interfaces on Equilibrium

$$\boldsymbol{\Delta G = \Delta P \cdot V} \Rightarrow \Delta G = \frac{2\gamma V_m}{r}$$

Extra pressure ΔP due to curvature of the **α/β**

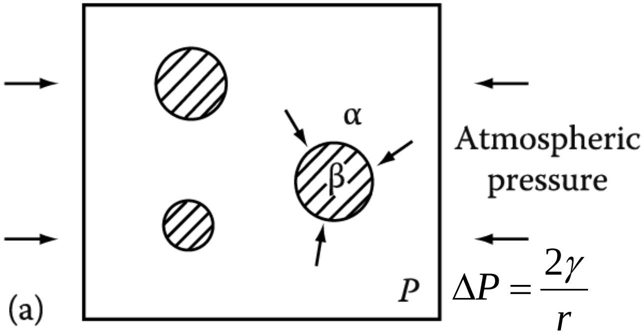

$$\Delta P = \frac{2\gamma}{r}$$

The concept of a pressure difference is very useful <u>for spherical liquid particles</u>, but it is less convenient in solids (often nonspherical shape).

$$\text{dG} = \boldsymbol{\Delta G_\gamma dn = \gamma dA} \qquad \boldsymbol{\Delta G_\gamma = \gamma dA/dn}$$

Since n=4πr³/3V$_m$ and A = 4πr² $\Delta G = \frac{2\gamma V_m}{r}$

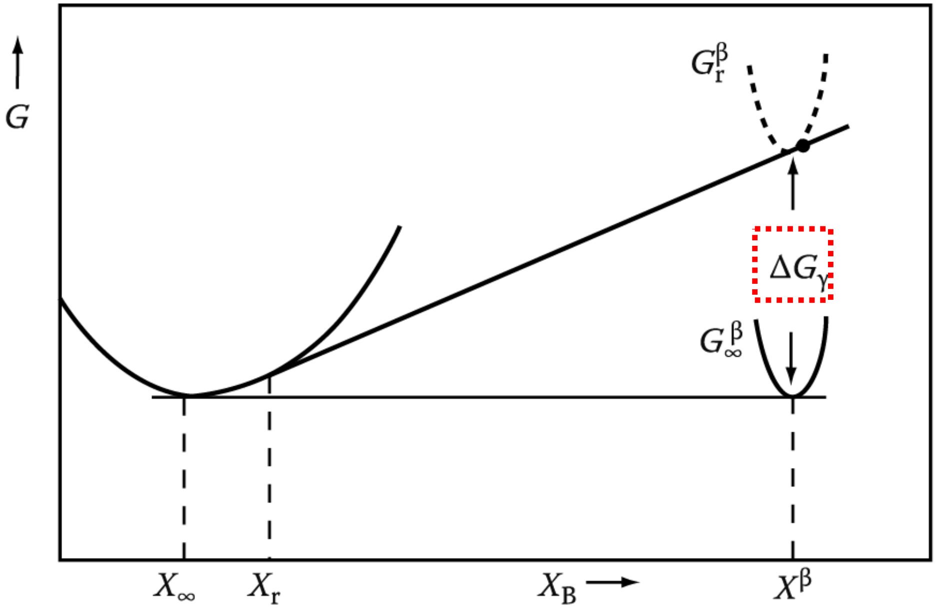

Fig. 1.38 The effect of interfacial E on the solubility of small particle

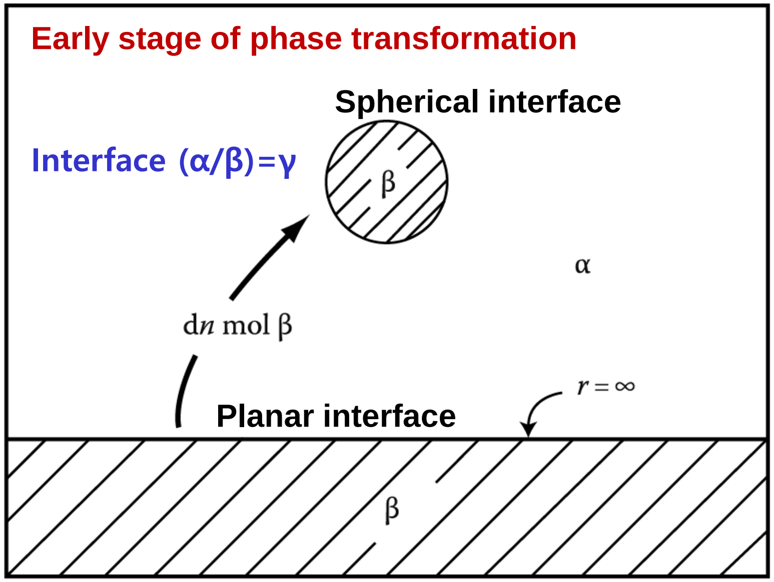

Fig. 1.39 Transfer of dn mol of β from large to a small particle.

$$\boxed{X_B^e = A\exp\left\{-\frac{Q}{RT}\right\}}$$

Gibbs-Thomson effect (capillarity effect):

Free energy increase due to interfacial energy

Quite large solubility differences can arise for particles in the range r=1-100 nm. However, for particles visible in the light microscope (r>1um) capillarity effects are very small.

$$X_B^e = \exp\left(-\frac{\Delta G_B + \Omega}{RT}\right)$$

$$X_B^{r=\infty} = \exp\left(-\frac{\Delta G_B + \Omega}{RT}\right)$$

$$X_B^{r=r} = \exp\left(-\frac{\Delta G_B + \Omega \boxed{- 2\gamma V_m / r}}{RT}\right)$$

$$= X_B^{r=\infty}\exp\left(\frac{2\gamma V_m}{RTr}\right)$$

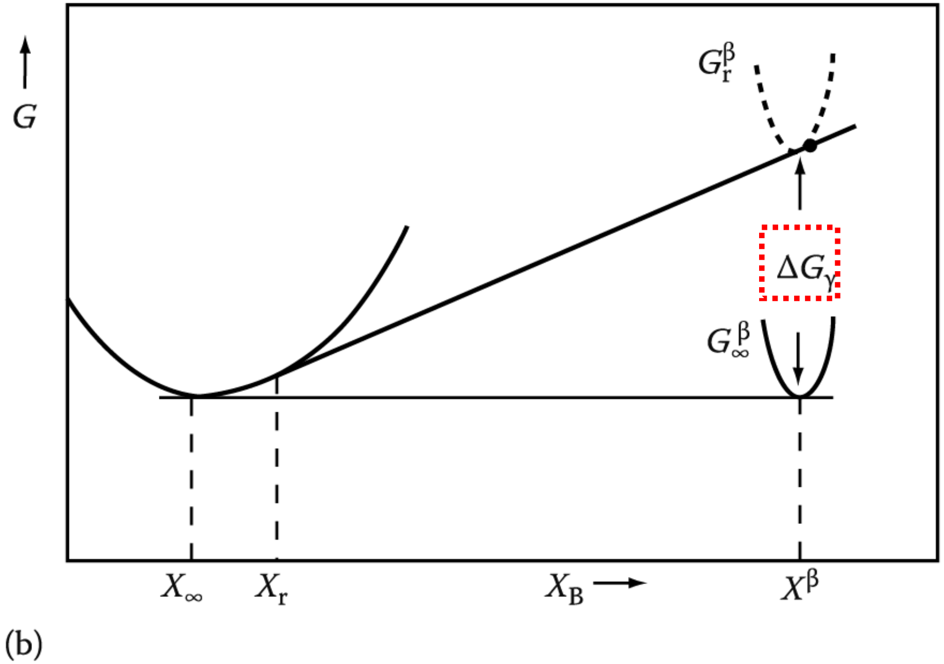

Fig. 1.38 The effect of interfacial energy on the solubility of small particles.

For small values of the exponent,

$$\frac{X_B^{r=r}}{X_B^{r=\infty}} = \exp\left(\frac{2\gamma V_m}{RTr}\right) \approx 1 + \frac{2\gamma V_m}{RTr}$$

Ex) **γ=200mJ/m², V_m=10⁻⁵ m³,T=500K**

$$\boxed{\frac{X_r}{X_\infty} = 1 + \frac{1}{r(nm)}}$$

For r=10 nm, solubility~10% increase

Microstructure of a two phase alloy is always unstable if the total interfacial free E is not a minimum. →

5.5.6. Particle Coarsening

(smaller total interfacial area→loss of strength or disappearance of GB pining effect→ particular concern in the design of materials for high temp. applications)

Two Adjacent Spherical Precipitates with Different Diameters

(Gibbs-Thomson effect: radius of curvature↓ → X_B ↑)

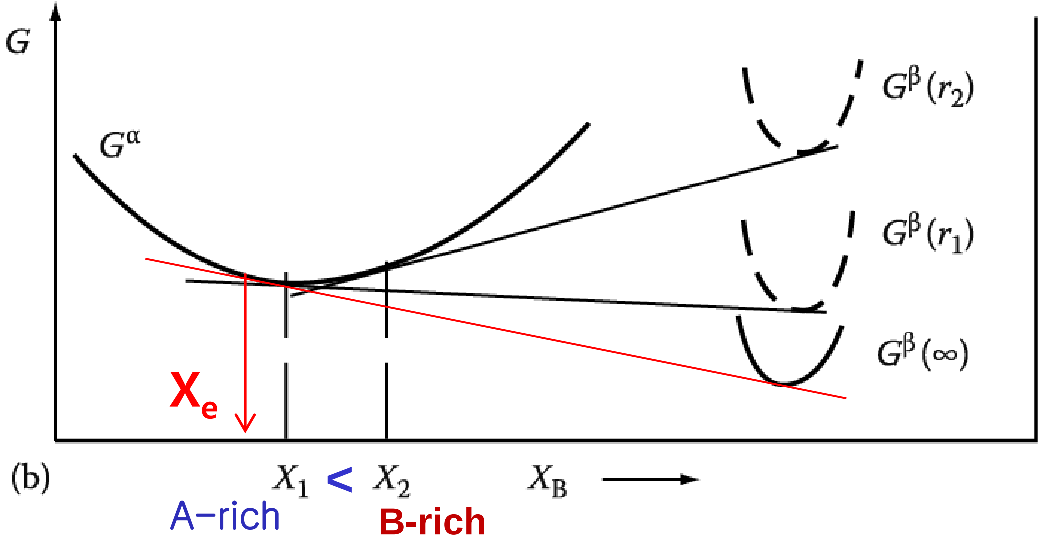

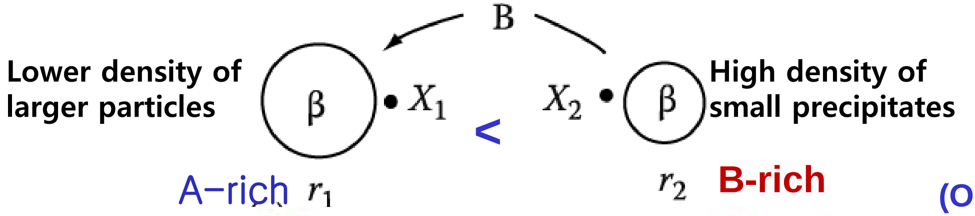

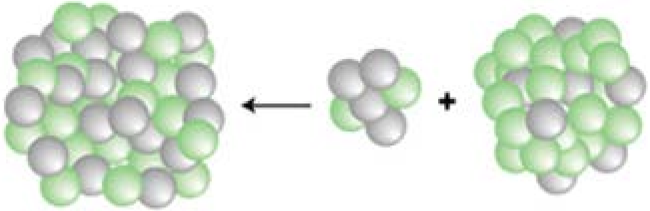

Assumption: volume diffusion is the rate controlling factor

$$(\bar{r})^3 - r_0^3 = kt$$

Average radius: $\bar{r}$

where $k \propto D\gamma X_e$

(X_e: Equil. solubility of very large particles)

Coarsening rate $$\boxed{\frac{d\bar{r}}{dt} \propto \frac{k}{\bar{r}^2}}$$

$$\left(\begin{array}{l} D \text{ and } X_e \sim \exp(-Q/RT) \uparrow \\ \bar{r} \downarrow \end{array}\right.$$

Rapidly increase with Increasing temp.

⇨ **CR** ↑

(Ostwald Ripening)

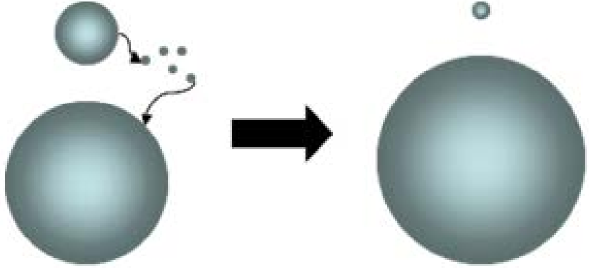

: Concentration gradient in matrix→diffusion→small particle_shrink/ large particle_grow

3.3 Calculation of critical radius

1) Assumption: solid ~ incompressible (two phases were at the same pressure),

$$T_E \rightarrow T_E - \Delta T,\ \Delta G_P\ (2\sigma/r^*) = \Delta P$$

$G^L = H^L - TS^L$

$G^S = H^S - TS^S$

$\Delta G_P = \Delta H - T\Delta S$

$L : \Delta H = H^L - H^S$

(Latent heat)

$T = T_E - \Delta T$

$\Delta G_P = 0 = \Delta H - T_E \Delta S$

$\Delta S = \Delta H / T_E = L / T_E$

$\Delta G_P = L - T(L/T_E) \approx (L\Delta T)/T_m$

$$\boxed{\Delta G_V = \Delta G_P = \frac{L\Delta T}{T_E}}$$

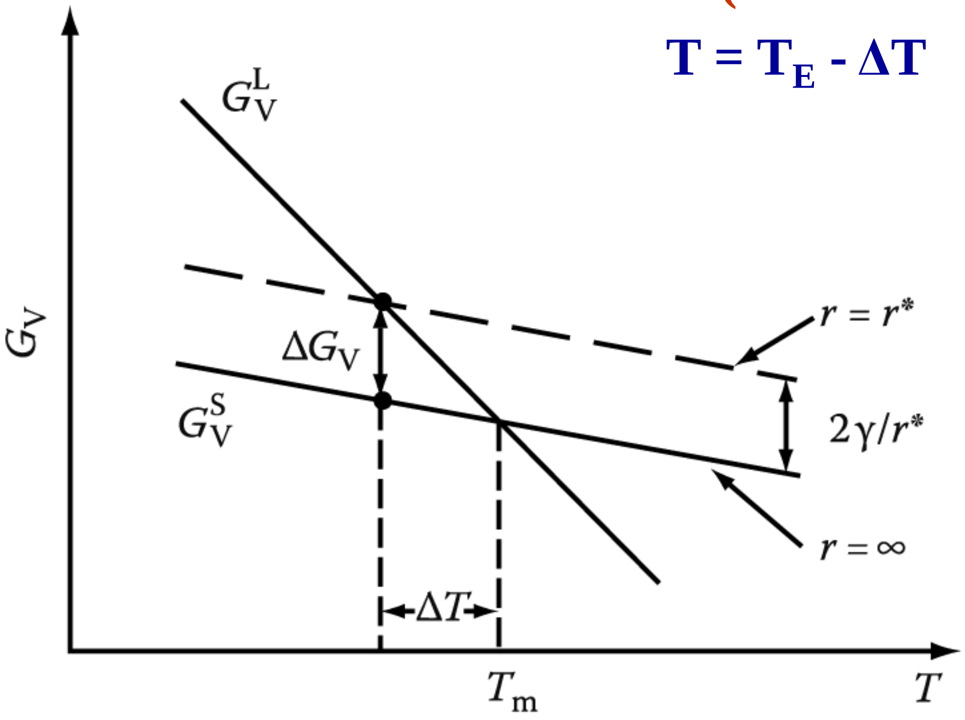

For incompressible solid,

$$\boxed{\frac{L\Delta T}{T_E} = \frac{2\sigma}{r^*}, \quad \text{or} \quad r^* = \frac{2\sigma T_E}{L\Delta T}}$$

ΔH, ΔS : independent of temperature

→ if the nucleation status is not incompressible, $\Delta G_P \not\approx \Delta P$

(ex. Nucleation of gas or vapor in liquid)

2) Calculation of critical radius II

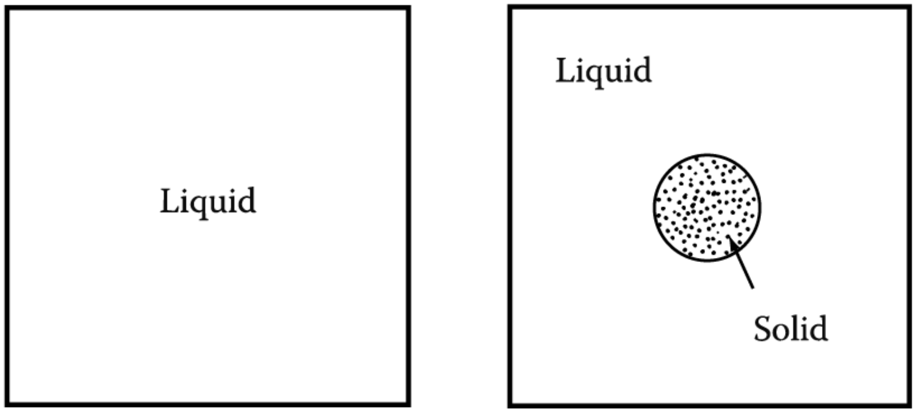

(a) G_1 (b) $G_2 = G_1 + \Delta G$

$$G_1 = (V_S + V_L)G_V^L$$

$$G_2 = V_S G_V^S + V_L G_V^L + A_{SL}\gamma_{SL}$$

G_V^S, G_V^L **: free energies per unit volume**

$$\Delta G = G_2 - G_1 = -V_S(G_V^L - G_V^S) + A_{SL}\gamma_{SL}$$

for spherical nuclei (isotropic) of radius : r

$$\boxed{\Delta G_r = -\frac{4}{3}\pi r^3 \Delta G_V + 4\pi r^2 \gamma_{SL}}$$

2) Calculation of critical radius II

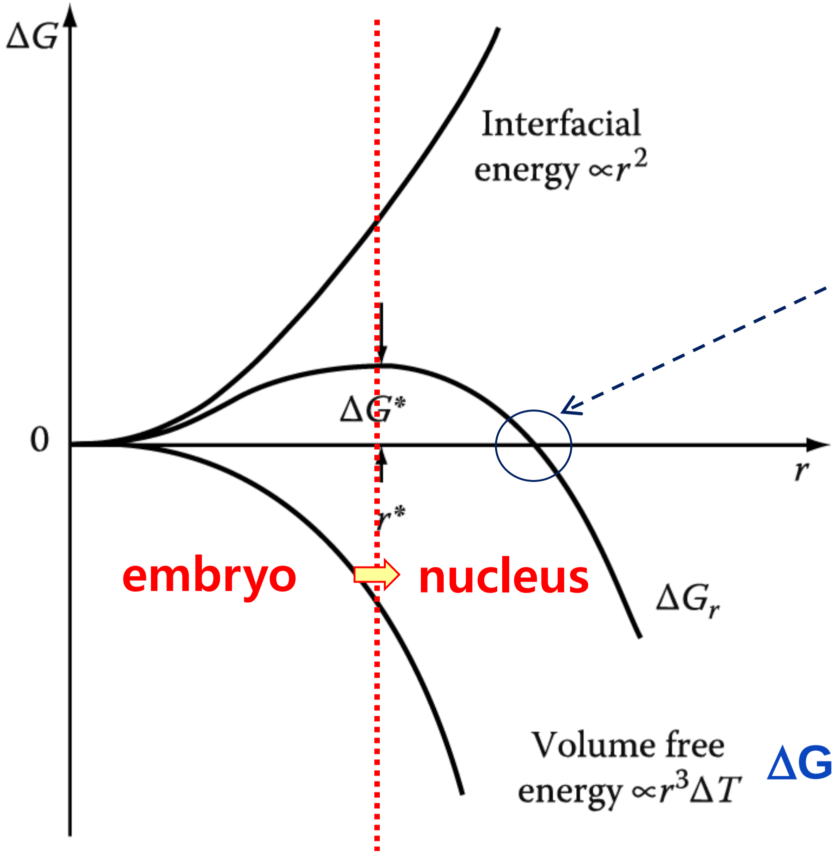

embryo ⇨ **nucleus**

$\Delta G_V = \Delta G_P$

Unstable equilibrium

Fig. 4. 2 The free energy change associated with homogeneous nucleation of a sphere of radius r.

$$\boxed{\Delta G_r = -\frac{4}{3}\pi r^3 \Delta G_V + 4\pi r^2 \gamma_{SL}}$$

Why r^* is not defined by $\Delta G_r = 0$?

$r < r^*$: unstable (lower free E by reduce size)

$r > r^*$: stable (lower free E by increase size)

r^* : critical nucleus size

$$r^* \Rightarrow dG=0$$

Gibbs-Thompson Equation

ΔG of a spherical particle of radius, r

$$\Delta G_{r(s)} = 4\pi r^2 \gamma$$

ΔG of a supersaturated solute in liquid in equilibrium with a particle of radius, r

$$\Delta G_{r(l)} = \frac{4\pi r^3}{3} \times \Delta G_V$$

Equil. condition for open system

⟶ Δμ should be the same.

$$\Delta\mu = 8\pi r \gamma = 4\pi r^2 \Delta G_V$$

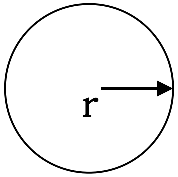

$\dfrac{2\gamma V_m}{r}$ **/mole or** $\dfrac{2\gamma}{r}$ **/ per unit volume**

$$\Delta G_V = 2\gamma_{SL} / r^*$$

r*: in (unstable) equilibrium with surrounding liquid

$$\boxed{r^* = \frac{2\gamma_{SL}}{\Delta G_V}} \Rightarrow \boxed{\Delta G^* = \frac{16\pi\gamma_{SL}^3}{3(\Delta G_V)^2} = \left(\frac{16\pi\gamma_{SL}^3 T_m^2}{3L_V^2}\right)\frac{1}{(\Delta T)^2}}$$

$$\boxed{\Delta G_r = -\frac{4}{3}\pi r^3 \Delta G_V + 4\pi r^2 \gamma_{SL}}$$

$$\boxed{\Delta G_V = \frac{L\Delta T}{T_m}}$$

- Critical condition of Nucleation → Depends on the curvature of the crystal surface
- To calculate r* under a given ΔT: $\sigma=\gamma_{SL}$ (Sol.-Liq. Interfacial E) measurement required

$$r^* = \frac{2\sigma T_E}{L\Delta T}$$

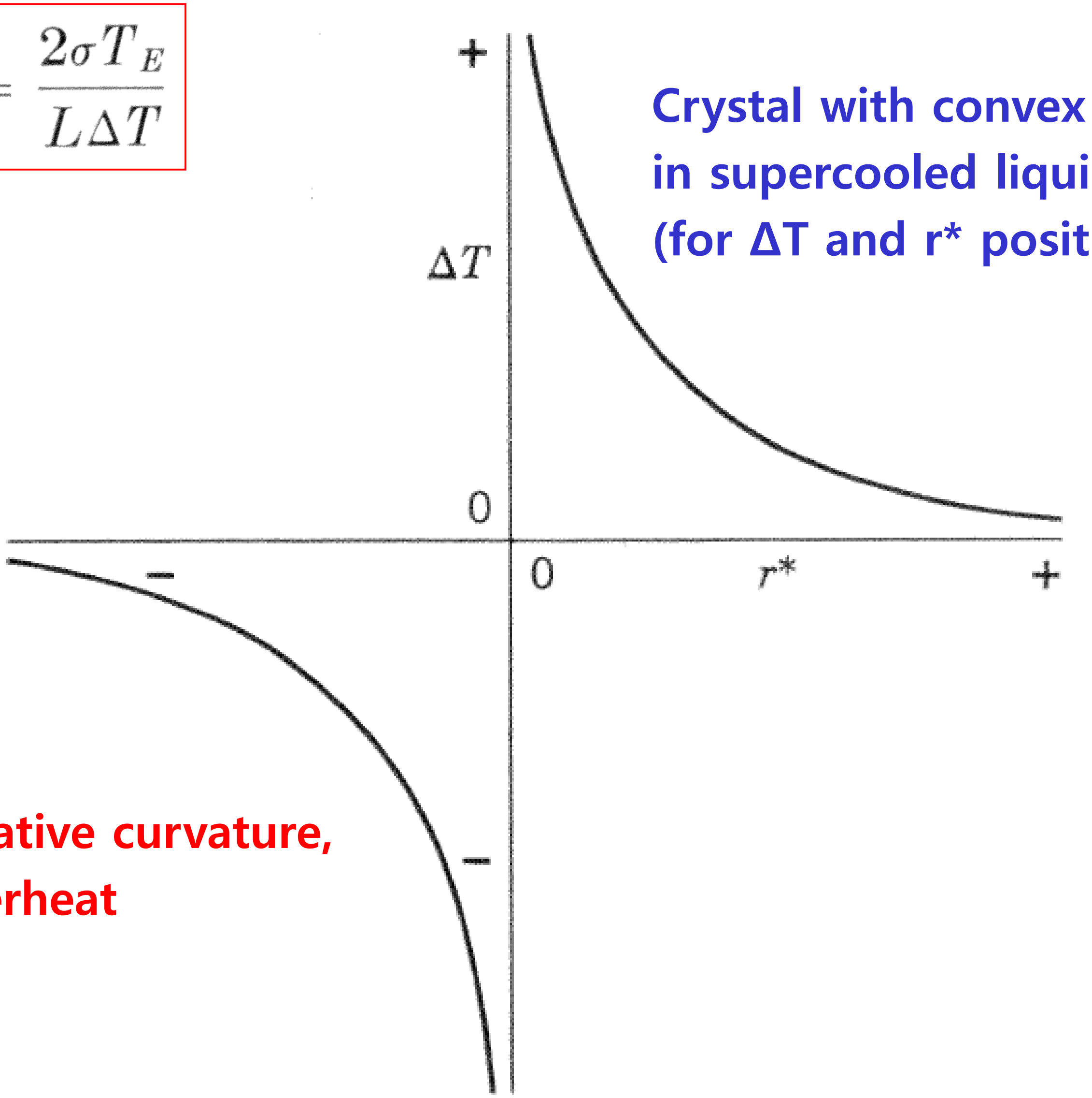

Crystal with convex surface in supercooled liquid (for ΔT and r* positive)

Negative curvature, superheat

Fig. 3.3. Relationship between critical radius and supercooling.

Formation of Atomic Cluster

At the T_m, the liquid phase has a volume 2-4% greater than the solid.

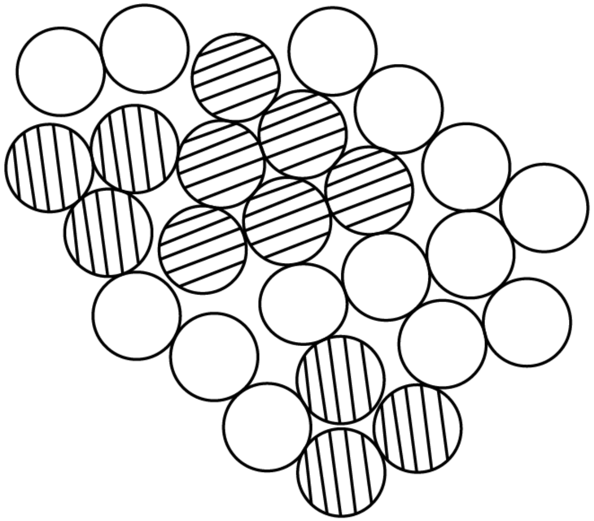

Fig. 4.4 **A two-dimensional representation of an instantaneous picture of the liquid structure. Many close-packed crystal-like clusters (shaded) are instantaneously formed.**

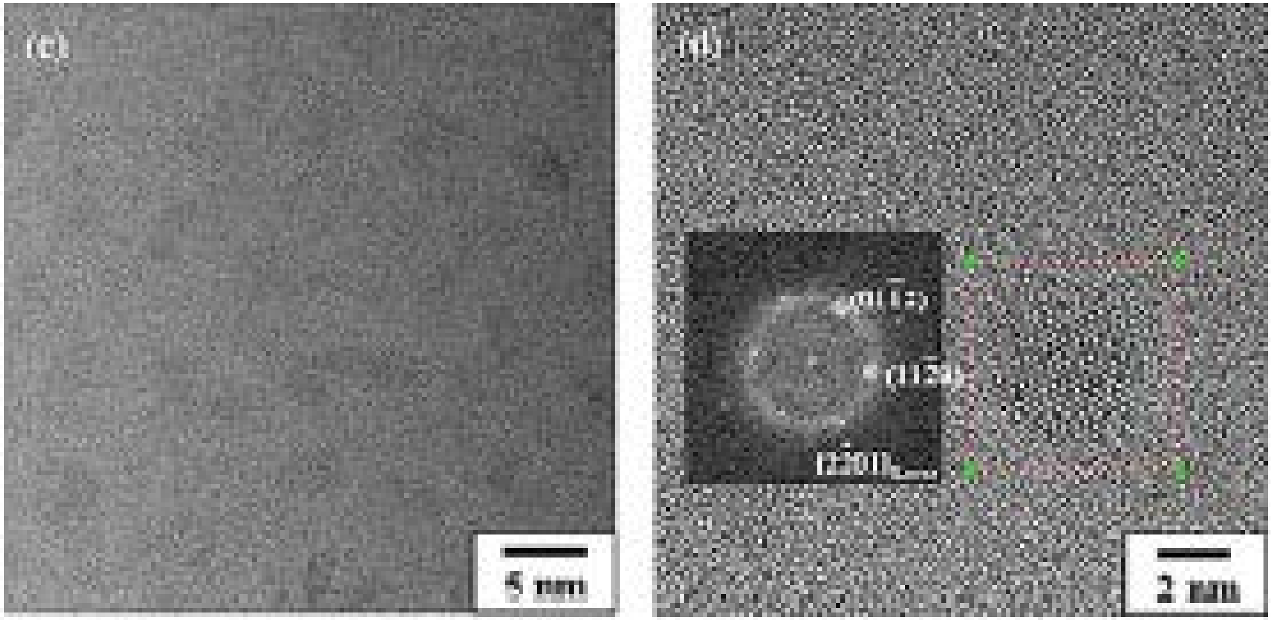

Formation of Atomic Cluster

When the free energy of the atomic cluster with radius r is by

$$\Delta G_r = -\frac{4}{3}\pi r^3 \Delta G_V + 4\pi r^2 \gamma_{SL},$$

how many atomic clusters of radius r would exist in the presence of the total number of atoms, n_0?

$$A_1 \to A_2 \to A_3 \to A_4 \to \cdots \to A_{m-1} \to A_m$$

$$n_2 = n_1 \exp\left(-\frac{\Delta G^{1\to 2}}{kT}\right)$$

Excess free E associated with the cluster of 1→2 atoms

$$n_3 = n_2 \exp\left(-\frac{\Delta G^{2\to 3}}{kT}\right)$$

$$n_4 = n_3 \exp\left(-\frac{\Delta G^{3\to 4}}{kT}\right)$$

$$\vdots$$

$$n_m = n_{m-1} \exp\left(-\frac{\Delta G^{m-1\to m}}{kT}\right)$$

$$n_m = n_1 \exp\left(-\frac{\Delta G^{1\to 2} + \Delta G^{2\to 3} + \cdots + \Delta G^{m-1\to m}}{kT}\right)$$

$$n_m = n_1 \exp\left(-\frac{\Delta G^{1\to m}}{kT}\right)$$

# of spherical clusters with radius r

# of cluster of radius r

$$n_r = n_0 \exp\left(-\frac{\Delta G_r}{kT}\right)$$

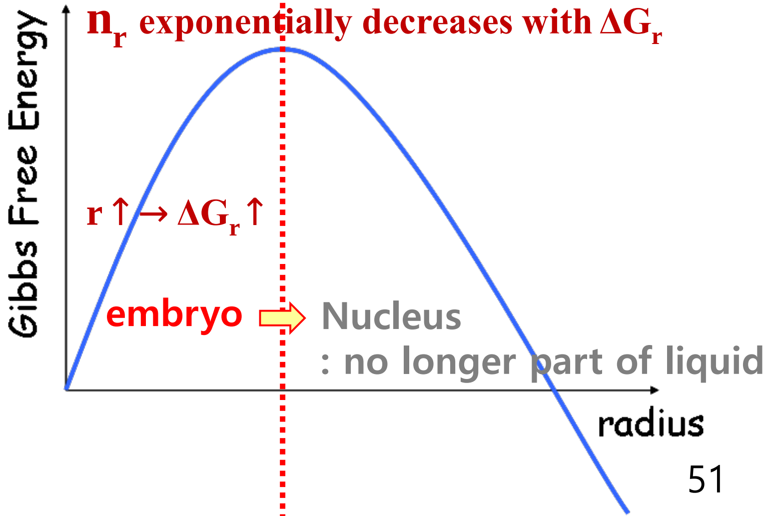

Formation of Atomic Cluster

Compare the nucleation curves between small and large driving forces.

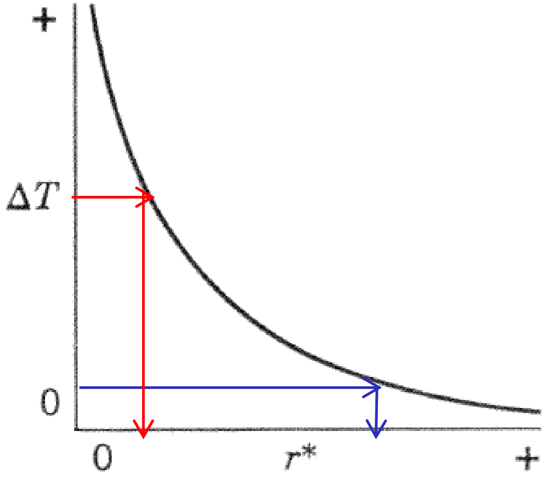

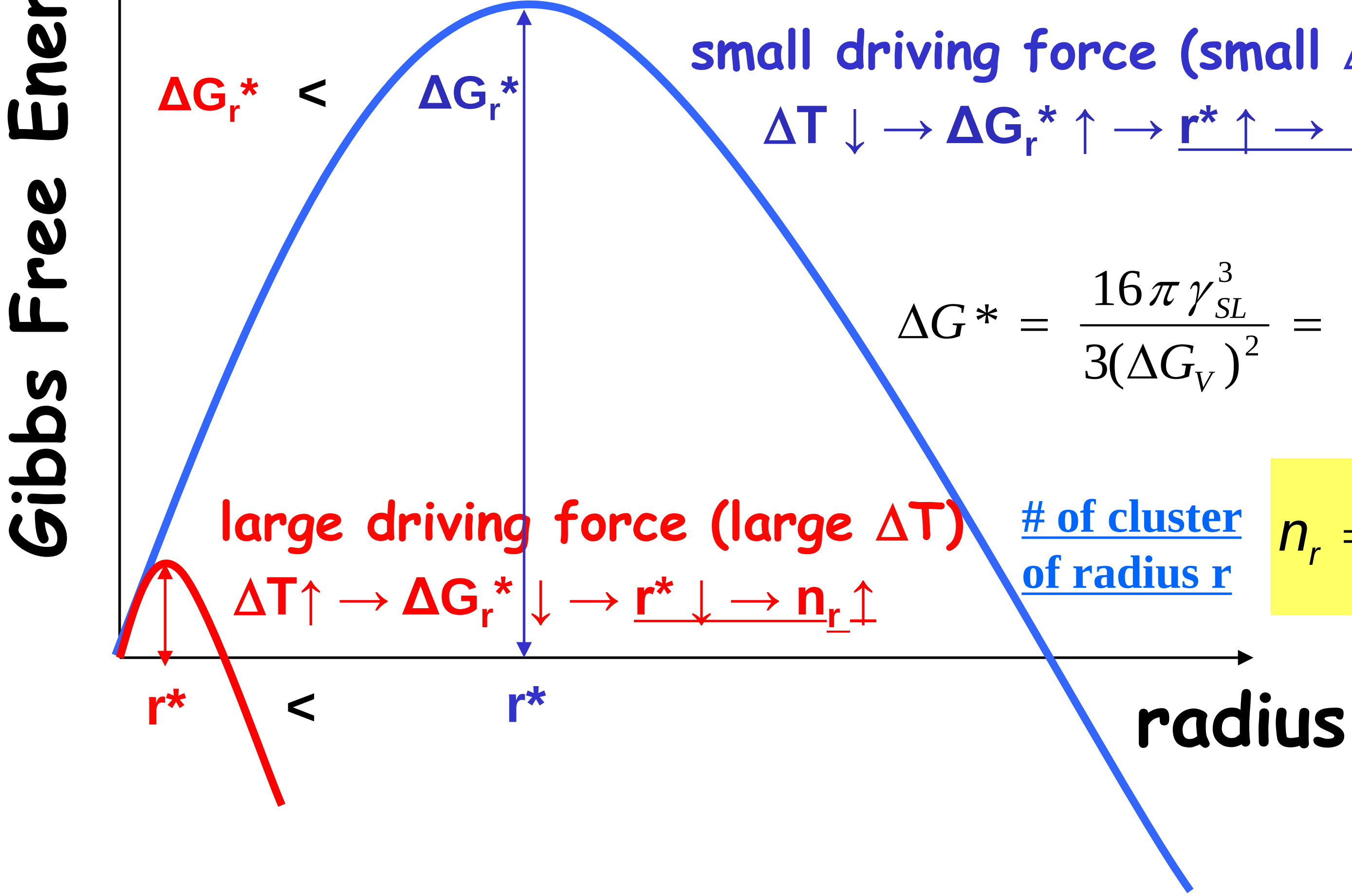

ΔG_r^* < ΔG_r^*

small driving force (small ΔT)

$\Delta T \downarrow \rightarrow \Delta G_r^* \uparrow \rightarrow \underline{r^* \uparrow \rightarrow n_r \downarrow}$

large driving force (large ΔT)

$\Delta T \uparrow \rightarrow \Delta G_r^* \downarrow \rightarrow \underline{r^* \downarrow \rightarrow n_r \uparrow}$

r^* < r^*

$$\Delta G^* = \frac{16\pi\gamma_{SL}^3}{3(\Delta G_V)^2} = \left(\frac{16\pi\gamma_{SL}^3 T_m^2}{3L_V^2}\right)\boxed{\frac{1}{(\Delta T)^2}}$$

<u>**# of cluster of radius r**</u>

$$n_r = n_0 \exp\left(-\frac{\Delta G_r}{kT}\right)$$

Formation of Atomic Cluster

n_o : total # of atoms.

ΔG_r : excess free energy associated with the cluster

k : Boltzmann's constant

# of cluster of radius r per unit volume

$$n_r = n_0 \exp\left(-\frac{\Delta G_r}{kT}\right)$$

- **$\Delta G_r \neq 0 \rightarrow n_r/n \neq 0$** (always cluster with a specific size)

→ **Key to nucleation : relationship btw r_{max} and r^***

- **holds for $T > T_m$ / $T < T_m$ and $r \leq r^*$**

Apply for all r / $r \leq r^*$

($\because$ $r > r^*$: no longer part of the liquid)

- **n_r exponentially decreases with ΔG_r**

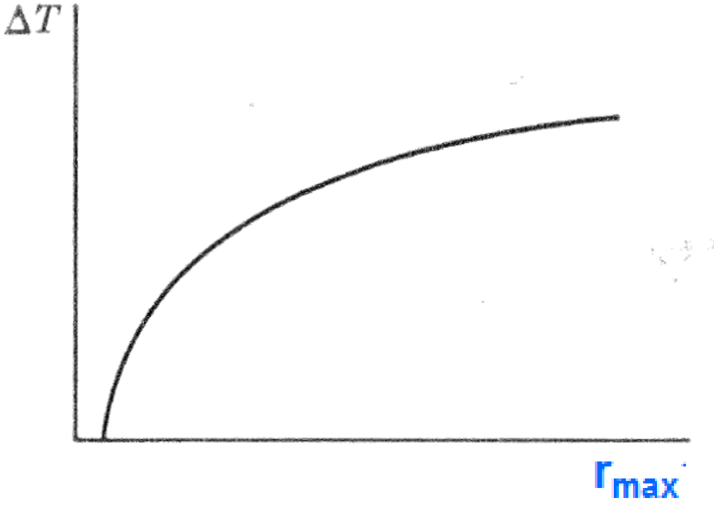

Fig. 3.5. Radius of largest embryo as a function of supercooling.

Ex. 1 mm^3 of copper at its melting point (n_0: 10^{20} atoms)

$r \downarrow \rightarrow n_r \uparrow$ → ~10^{14} clusters of 0.3 nm radius (i.e. ~ 10 atoms)

$r \uparrow \rightarrow n_r \downarrow$ → ~10 clusters of 0.6 nm radius (i.e. ~ 60 atoms)

→ effectively a maximum cluster size, ~ 100 atoms

~ 10^{-8} clusters mm^{-3} or 1 cluster in ~ 10^7 mm^3

The creation of a critical nucleus ~ thermally activated process

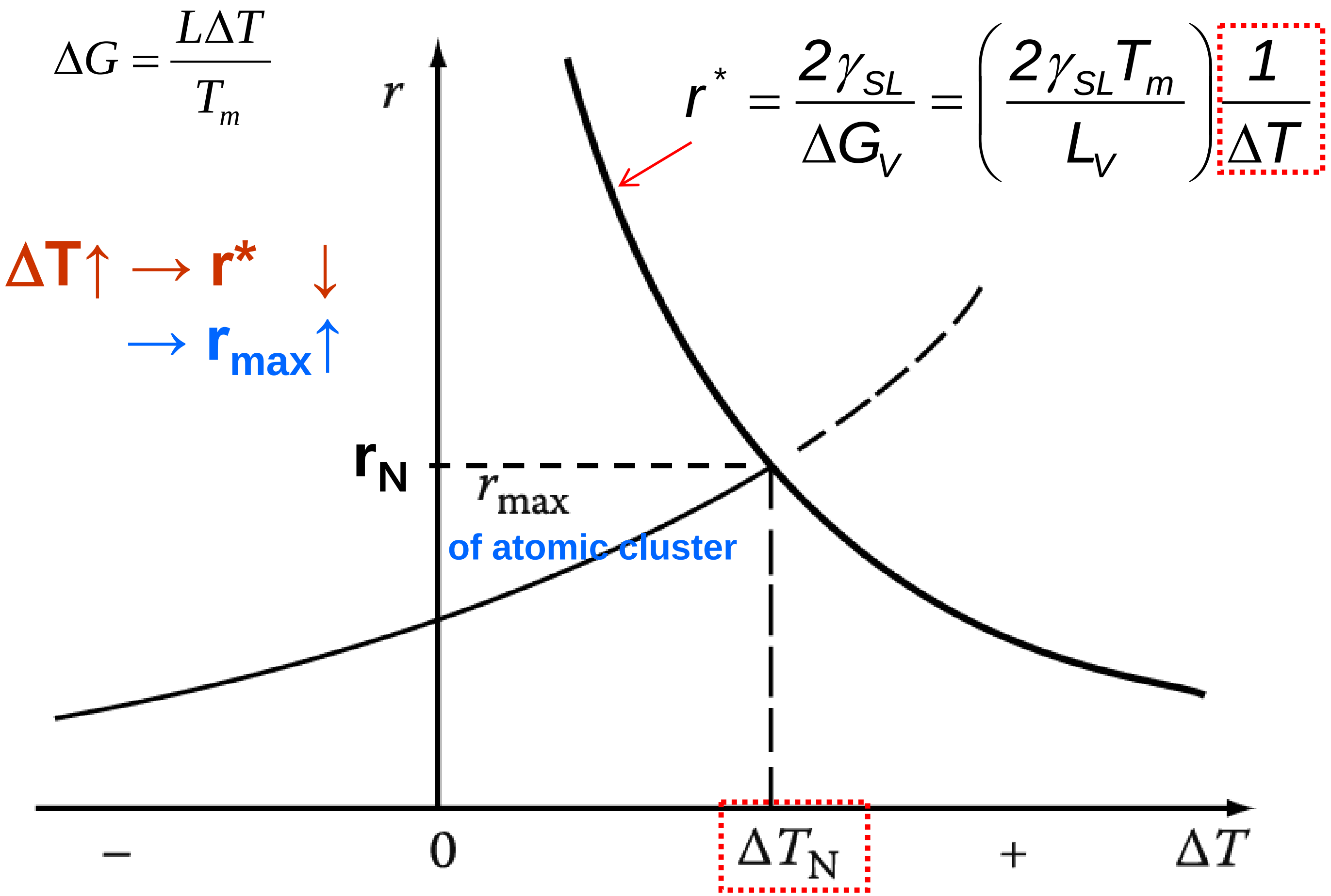

$$\Delta G = \frac{L \Delta T}{T_m}$$

$$r^* = \frac{2\gamma_{SL}}{\Delta G_V} = \left(\frac{2\gamma_{SL} T_m}{L_V} \right) \boxed{\frac{1}{\Delta T}}$$

$\Delta T \uparrow \rightarrow r^* \downarrow$

$\rightarrow r_{max} \uparrow$

ΔT_N is the critical undercooling for homogeneous nucleation.

The variation of r* and r_{max} with undercooling ΔT

→ The condition for nucleation:

The number of clusters with r^* at $T < \Delta T_N$ is negligible.

2) The homogeneous nucleation rate - kinetics

How fast solid nuclei will appear in the liquid at a given undercooling?

n : atoms/unit volume
n_i^* : # of clusters with size of r* (critical size)

$$n_i^* = n \exp\left(-\frac{\Delta G^*}{kT}\right)$$ **clusters / m³**

$\Delta G^* = 16\pi\sigma^3/(\Delta G_P)^2$

Excess free E of critical nucleus

The addition of one more atom to each of these clusters will convert them into stable nuclei.

Homogeneous nucleation rate
(small embryos → r*)

$$N_{hom} = I = ZS^* n_i^*$$ **nuclei / m³·s**

Net rate at which atoms travel across the interface btw liquid and embryo

Surface area of Critical nucleus

Equilibrium # of Critical nuclei

2) The homogeneous nucleation rate - kinetics

$$I = K_v \exp\{-[(\Delta G^* + \Delta G_A)kT]\}$$

$$K_v = n^*(a\sigma/9\pi kT)^{1/2}n(kT/h)$$

a: correction factor of nucleus shape (Not necessarily spheircal)
n∗: # of surface atoms for critical nucleus
n = # of atoms per unit volume for liquid

Assumption: **“equilibrium distribution of the embryo size at all times” (ideal condition)**
Vapor → liquid drop : OK but liquid → Solid : X due to low mobility

$$I = \frac{nkT}{h}\exp\left(-\frac{G_A}{kT}\right)\exp\left(-\frac{16\pi\sigma_{SL}{}^3T_E{}^2}{3L^2(\Delta T)^2kT}\right)$$

→ Until ΔT reaches, the critical value *I* is very small.

But ΔT increases rapidly when critical value is reached

The homogeneous nucleation rate - kinetics

$$I = \frac{nkT}{h}\exp\left(-\frac{G_A}{kT}\right)\exp\left(-\frac{16\pi\sigma_{SL}{}^3T_E{}^2}{3L^2(\Delta T)^2kT}\right)$$

: insensitive to Temp.

How do we define nucleation temperature, ΔT_N ?

$$\boxed{N_{\mathrm{hom}} \sim \frac{1}{\Delta T^2}}$$

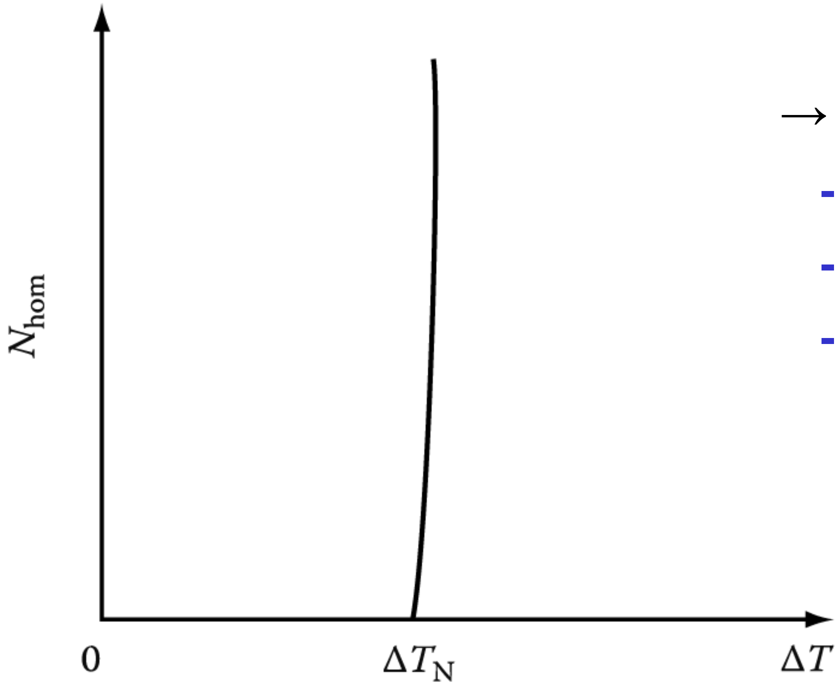

→ **critical value for detectable nucleation**

- **critical supersaturation ratio**
- **critical driving force**
- **critical supercooling**

→ **for most metals, ΔT_N~0.2 T_m (i.e. ~200K)**

The homogeneous nucleation rate as a function of undercooling ΔT. ΔT_N is the critical undercooling for homogeneous nucleation.

* Comparison between experiment and theory

Most metal ΔT_N < several K

but Turnbull and his coworker ΔT_N → larger (~several hundreds K)

by formation of large number of very small drops

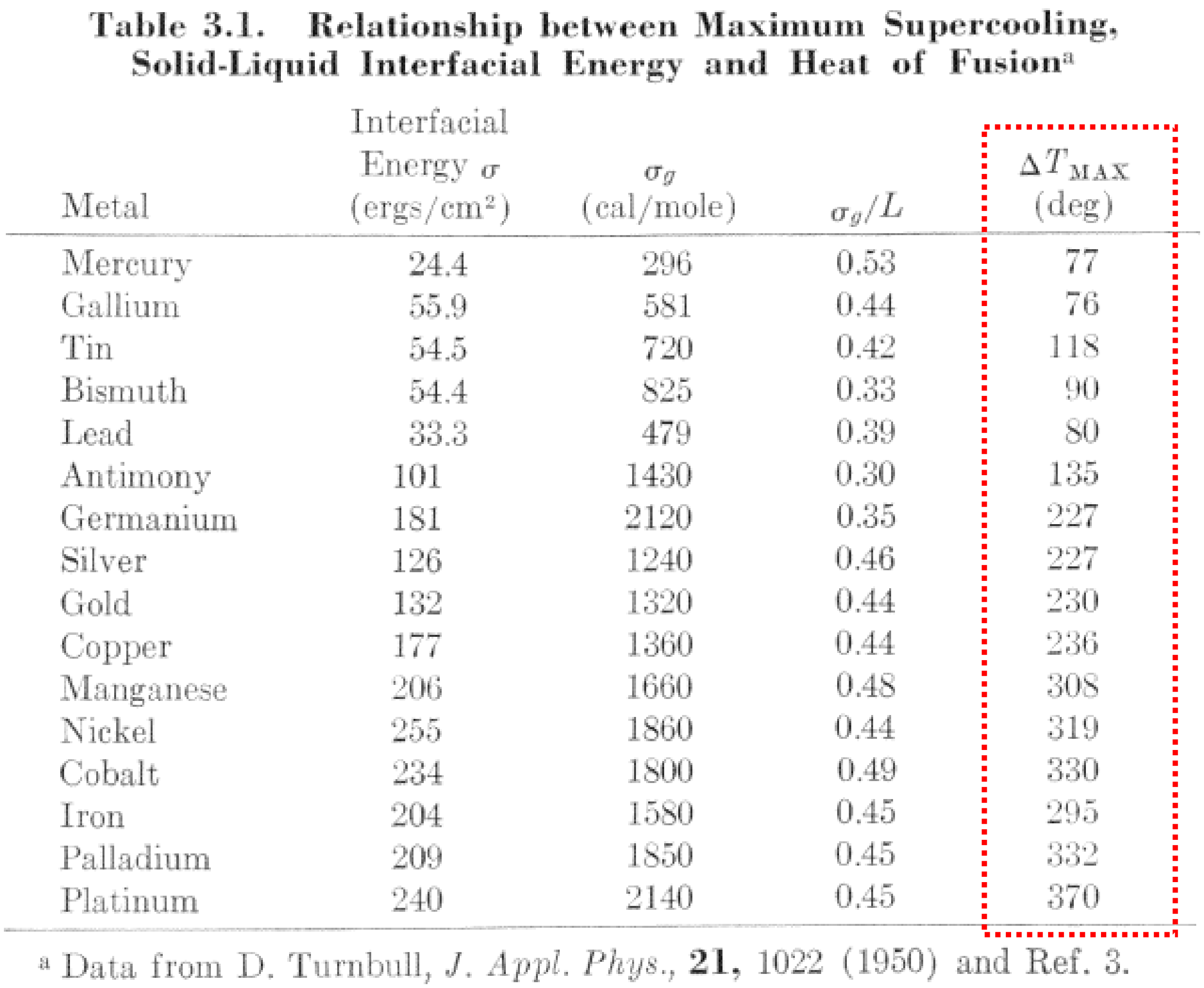

Table 3.1. Relationship between Maximum Supercooling, Solid-Liquid Interfacial Energy and Heat of Fusion[a]

Metal	Interfacial Energy σ (ergs/cm²)	σ_g (cal/mole)	σ_g/L	ΔT_{MAX} (deg)
Mercury	24.4	296	0.53	77
Gallium	55.9	581	0.44	76
Tin	54.5	720	0.42	118
Bismuth	54.4	825	0.33	90
Lead	33.3	479	0.39	80
Antimony	101	1430	0.30	135
Germanium	181	2120	0.35	227
Silver	126	1240	0.46	227
Gold	132	1320	0.44	230
Copper	177	1360	0.44	236
Manganese	206	1660	0.48	308
Nickel	255	1860	0.44	319
Cobalt	234	1800	0.49	330
Iron	204	1580	0.45	295
Palladium	209	1850	0.45	332
Platinum	240	2140	0.45	370

[a] Data from D. Turnbull, *J. Appl. Phys.*, **21**, 1022 (1950) and Ref. 3.

How to Obtain Extensive Undercooling

John H. PEREPEZKO, MSE, 65 (1984) 125-135

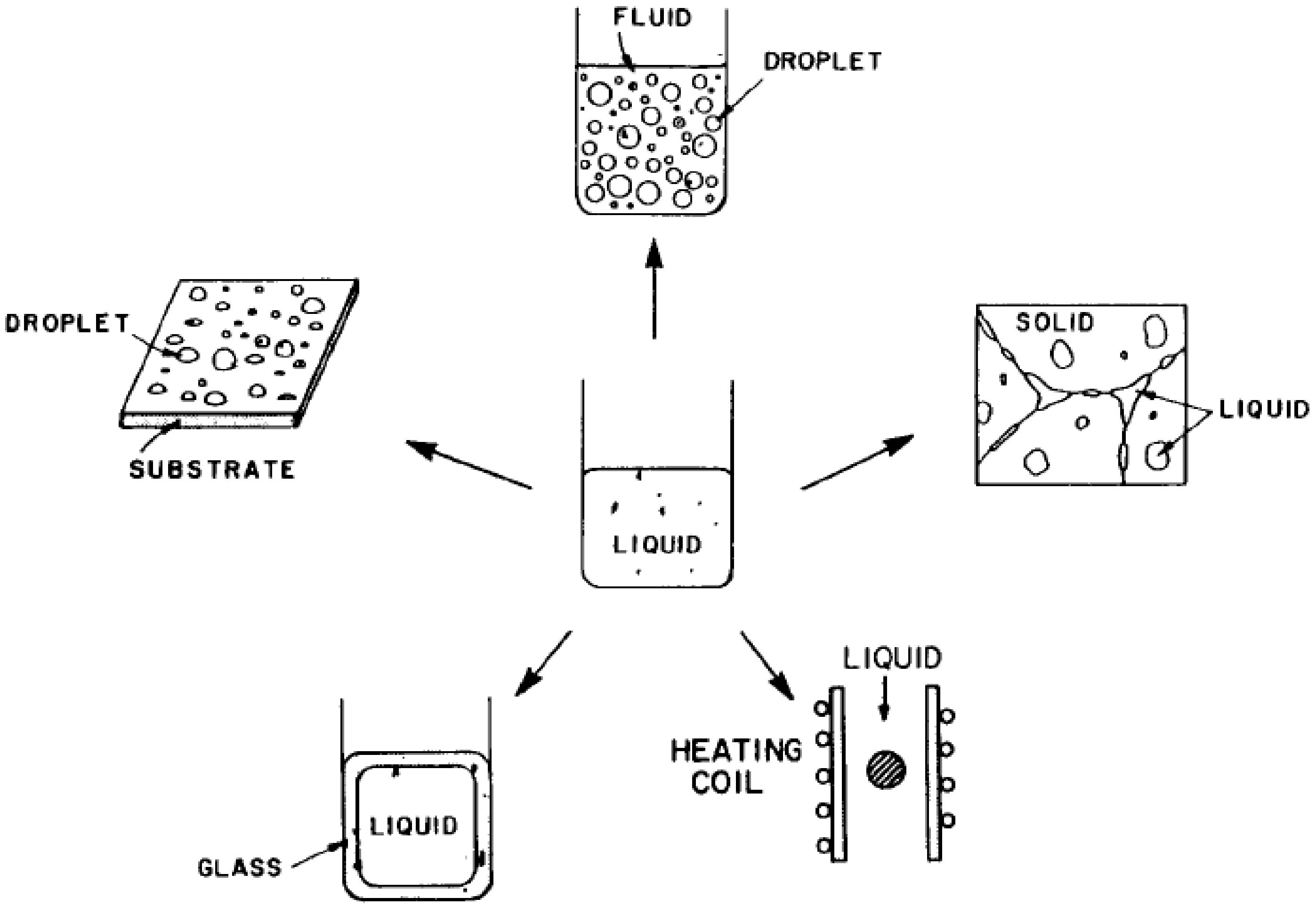

By dispersing a liquid into a large number of small droplets within a suitable medium, the catalytic effects of active nucleants may be restricted to a small fraction of the droplets so that many droplets will exhibit extensive undercooling.

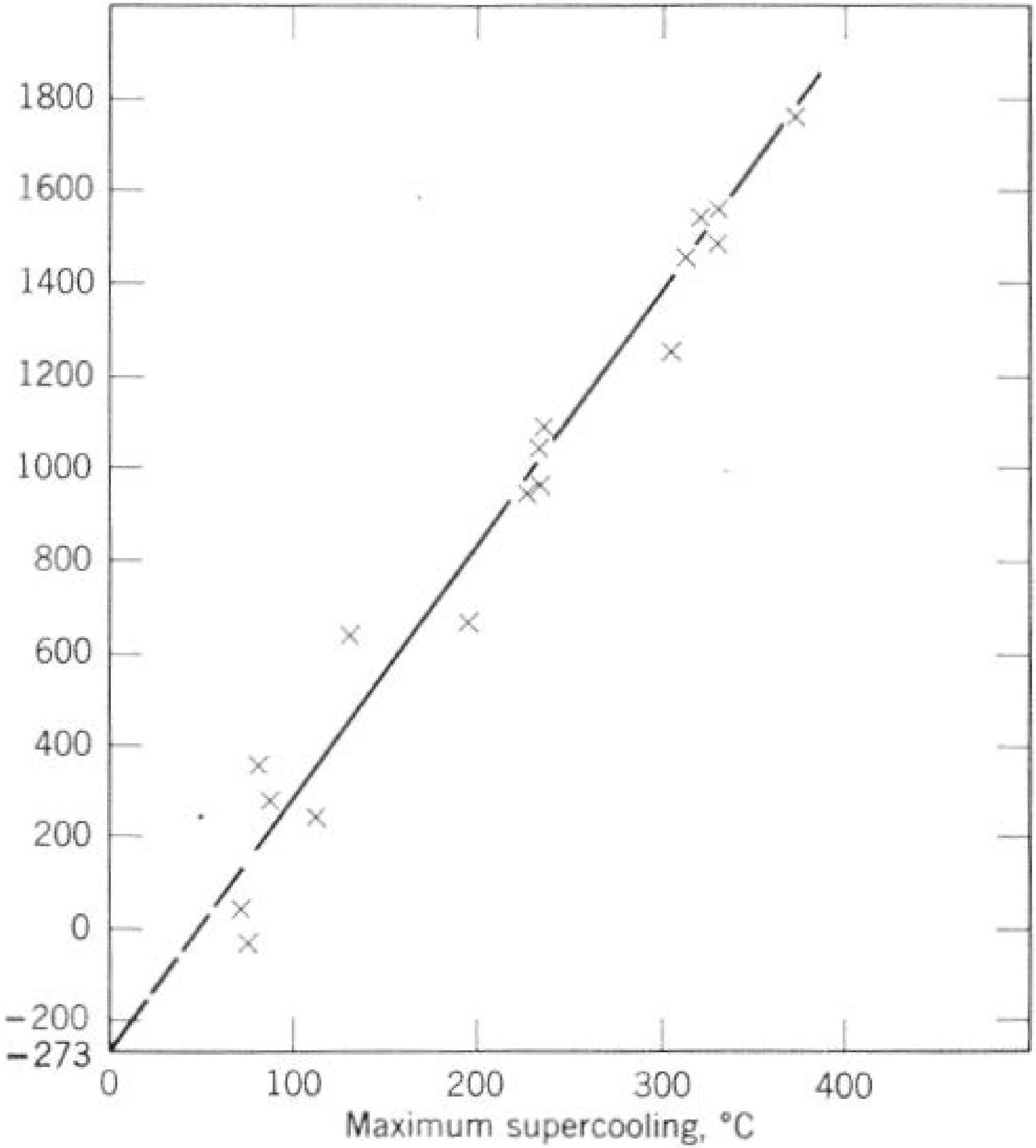

Fig. 3.7. Maximum supercooling as a function of melting point. (From *Thermodynamics in Physical Metallurgy*, American Society for Metals, Cleveland, 1911, p. 11.)

Maximum undercooling vs. Melting temperature